Available online at http://scik.org
Commun. Math. Biol. Neurosci. 2023, 2023:99
https://doi.org/10.28919/cmbn/8164
ISSN: 2052-2541

CONTRIBUTION OF HUNTING COOPERATION AND ANTIPREDATOR BEHAVIOR TO THE DYNAMICS OF THE HARVESTED PREY-PREDATOR SYSTEM

RAID KAMEL NAJI*

Department of Mathematics, College of Science, University of Baghdad, Baghdad, Iraq

Abstract: Fear, harvesting, hunting cooperation, and antipredator behavior are all important subjects in ecology. As a result, a modified Leslie-Gower prey-predator model containing these biological aspects is mathematically constructed, when the predation processes are described using the Beddington-DeAngelis type of functional response. The solution's positivity and boundedness are studied. The qualitative characteristics of the model are explored, including stability, persistence, and bifurcation analysis. To verify the gained theoretical findings and comprehend the consequences of modifying the system's parameters on their dynamical behavior, a detailed numerical investigation is carried out using MATLAB and Mathematica. It is discovered that the presence of these components enriches the system's dynamic behavior, resulting in bi-stable behavior.

Keywords: prey-predator; fear; hunting cooperation; antipredator behavior; stability; persistence; bifurcation.

2020 AMS Subject Classification: 92D40, 92D30, 34D20, 34C23.

---

*Corresponding author
E-mail address: rknaji@gmail.com
Received August 05, 2023

1. INTRODUCTION

One of the prominent themes in Mathematical Ecology, and particularly in Population Dynamics, has been and remains to be the dynamic interplay between predators and their prey. This is due to its universality, as well as the fact that a more comprehensive understanding of this relationship allows for a better understanding of the movement of food chains or trophic webs. The first prey-predator model, defined by an autonomous nonlinear ODE system, was proposed by the Italian scientist Vito Volterra in 1926. This model corresponded to a two-dimensional model for biological interactions published previously by American scientist Alfred J. Lotka; for the aforementioned, the ODE system is known as the Lotka-Volterra model [1-2]. The primary dynamic feature of this first prey-predator model is that the single point of positive equilibrium is a center, implying that all pathways are concentric closed orbits around that point [3-4]. This indicates that given any beginning state, the density size of predators and their prey would continually swing about that point. This behavior of the system solutions was fiercely questioned when they were developed because no prey-predator interactions with these features were seen in nature.

The model developed by British scientist Leslie in 1948 offers a new alternative that does not suit the Lotka-Volterra model scheme, which is based on a notion of mass or energy transfer, the Leslie model distinguishes itself because the predator growth equation, like the prey growth equation, is of the logistic type. Leslie assumed that the predators' traditional ecological carrying capacity relates to the abundance of prey $K(N) = aN$, where N denotes prey density [5]. When a predator is a generalist and no preferred prey exists, the predator may shift to another food source. In this scenario, $K(N) = aN + K$, where $K > 0$ denotes the quantity of other nourishment available to predators or predator carrying capacity in the absence of the prey. As a result, an improved Leslie-Gower system or a Leslie-Gower strategy is produced [6]. Subsequently, these systems' applications began to expand. New population dynamics applications have been developed, and these systems had been used to simulate a range of other natural phenomena, see [7-10] and the references therein.

Many prey species adjust their behavior in the presence of predators due to predation risk and exhibit a variety of antipredator responses, which include foraging activity, habitat adaptations, vigilance, and some physiological changes, among other things [11-13]. Many researchers have discovered that fear of predation reduces the reproduction of fearful victims. Recently, fear has been studied extensively in basic ecology and environmental biology, see [14–22] and the references therein. Harvesting, on the other hand, is a significant and frequent occurrence. Because ecosystems are primarily regenerative, fishermen commonly employ harvesting. Scientists are investigating the capture of either prey or predator species, or both prey and predator species, in a capitalized hunting system with two interacting species. Many alternative harvesting methods have been employed. Continuous threshold harvesting, proportional harvesting, and constant harvesting are used by some [23-25], whereas nonlinear harvesting is investigated by others [8-10, 26].

Lately, Alves and Hilker [27] investigated predator hunting cooperation, believing that predators gain from their cooperative behaviors so that the quantity of prey attacks rises with predator density, and demonstrated numerically how levels of their hunting cooperation impact predator density, predator existence, and ecosystem stability. They defined the Holling type-I functional response as $f(N,P) = (a + hP)N$, where $h > 0$ represents predator cooperation in hunting and $a > 0$ represents the attack rate per predator and prey so that cooperation term was hP. When compared to the condition of no hunting cooperation, they discovered that hunting cooperation substantially mediates predator existence and causes oscillatory behaviors. Recently, many researchers have investigated the ecological systems in the existence of hunting cooperation to understand their effects on the system dynamic, see [28-31] and the references therein.

In response to the above discussion, we created a modified Leslie-Gower prey-predator model that takes into account the effects of fear on prey reproduction and their environment-carrying capacity. It also considers nonlinear harvesting, hunting cooperation, and predator behavior. The consumption process is described using the Beddington–DeAngelis kind of functional response. The following is how this work is organized. The mathematical model is developed in the next section. Section 3 focuses on the system's stability. Section 4 investigates the system's uniform persistence. Section 5 determines the conditions for the occurrence of local bifurcation. We performed various numerical simulations to demonstrate our theoretical findings, which are described in Section 6. Finally, Section 7 discusses the study's findings.

2. CONSTRUCTION OF THE MODEL

In this section, a prey-predator model with a generalist predator is formulated, indicating it can live without the model's prey population. Hence, it has an alternate food source. This suggests that the per capita growth rate function will be zero at some positive density. The simplest situation is when we describe the dynamics of a predator population using logistic growth in the absence of prey. Taking the simplest version of the predator population's growth rate, the Leslie–Gower prey-predator [5] with logistic growth in both prey and predator and general functional response is described as [32]

$$\begin{aligned} \frac{dN}{dT} &= rN\left(1-\frac{N}{K}\right)-\frac{qNP}{p+N} \\ \frac{dP}{dT} &= sP\left(1-\frac{P}{hN}\right) \end{aligned} \tag{1}$$

In this case, $N(T)>0$ and $P(T)>0$ are utilized to represent the magnitude of the prey and predator populations at time T. With carrying capacity K and intrinsic growth rate r, the prey population grows logistically. The predator's growth is also logistic, with an intrinsic growth rate s. Nonetheless, carrying capacity is prey-dependent, with h indicating the importance of the prey as food for the predator. The term $\frac{P}{hN}$ is called the Leslie-Gower term.

On the other hand, predators can consume other populations when food is short, but their expansion will be limited because their preferred prey is rare. To address this issue, Aziz-Alaoui and Okiye [6] proposed a modified Leslie-Gower model in which a constant b is introduced into the denominator of the Leslie-Gower term that assesses ecological safeguards for the predator in order to avoid singularities when $N=0$, so that system (1) becomes

$$\begin{aligned} \frac{dN}{dT} &= rN\left(1-\frac{N}{K}\right)-\frac{qNP}{p+N} \\ \frac{dP}{dT} &= sP\left(1-\frac{P}{b+hN}\right) \end{aligned} \tag{2}$$

Many researchers have now investigated the modified Leslie-Gower models incorporating many different kinds of functional responses, harvesting, the Allee effect [8, 33-36], and so on.

The modified Leslie–Gower prey-predator model (2) with the Sarkar and Khajanchi fear function [37] that influences the prey's birth rate and the quadratic fixed effort harvesting with the Beddington–DeAngelis type of functional response is proposed and investigated by Jamil and Naji, [9] in the following form:

$$\begin{aligned} \frac{dN}{dT} &= N\left[r_1\left(m+\frac{n(1-m)}{n+P}\right)-d-bN-\frac{aP}{c+N+eP}-q_1EN\right], \\ \frac{dP}{dT} &= P\left[r_2\left(1-\frac{P}{K+N}\right)-q_2EP\right], \end{aligned} \tag{3}$$

Because of the significance of the prey's refuge, prey refugees are assumed to minimize predator-prey fluctuations and prevent prey extinction [10]. A review of the real-world proof suggests that refuges can perform the former purpose. As a result, in the aforementioned dynamical model, the overall amount of prey refuge is dependent on both species. Assume that the amount of prey refuge is δNP [38], where δ is the refuge coefficient. Therefore, the predators prey on the remaining $(N-\delta NP)$ prey species, where $0<\delta<1$. Accordingly, the dynamics of the above-described model can be written as [27].

$$\begin{aligned} \frac{dN}{dT} &= N\left[r_1\left(m+\frac{n(1-m)}{n+P}\right)-d-bN-\frac{a(1-\delta P)P}{c+N(1-\delta P)+eP}-q_1EN\right], \\ \frac{dP}{dT} &= P\left[r_2\left(1-\frac{P}{K+(1-\delta P)N}\right)-q_2EP\right], \end{aligned} \tag{4}$$

Keeping the above in view, this paper considers the influence of hunting cooperation on the model (3) instead of predator-dependent refuge with antipredator behavior, which can be seen in real-world life between wild buffalo and lions. Consequently, the modified Leslie–Gower prey-predator system that has hunting cooperation and antipredator behavior can be represented using the following set of differential equations.

$$\begin{aligned} \frac{dN}{dT} &= N\left[r_1\left(m+\frac{n(1-m)}{n+P}\right)-d_1-bN-\frac{(a+hP)P}{c_1+(a+hP)N+c_2P}-q_1EN\right]=Nf(N,P), \\ \frac{dP}{dT} &= P\left[r_2\left(1-\frac{P}{K+(a+hP)N}\right)-d_2\mathrm{N}-q_2EP\right]=Pg(N,P), \end{aligned} \tag{5}$$

where all the parameters are nonnegative and described in Table 1.

Table 1. Parameters' description.

Parameter	Description
r_1, r_2	The birth rate of the prey population and predator population, respectively.
m	The minimum cost of fear with $m \in [0,1]$.
n	The level of fear.
d_1	The natural death rate of the prey.
d_2	The antipredator rate.
b	Decay rate due to intraspecific competition.
a	The attack rate.
h	The Hunting cooperation rate.
c_1	Half saturation constant.
c_2	A level of interference between the individuals of a predator.
q_1, q_2	The catchability coefficients of the prey and predator, respectively.
E	The effort level for harvesting the prey and predator.
K	The carrying capacity of the predator in the absence of its prey.

According to the interaction functions $f(N,P)$ and $g(N,P)$, the right-hand side functions of the system (5) are continuous and have continuous partial derivatives, therefore these functions are Lipschitzain. Consequently, depending on the fundamental theorem of existence and uniqueness for the solution of the initial value problems, system (5) with the initial condition $N(0) \geq 0$, and $P(0) \geq 0$ have a unique solution.

Theorem 1. System (5) is a positively invariant system.

Proof. The form of System (5) indicates that the system is a Kolmogorov system, with $f(N,P)$ and $g(N,P)$ being continuously differentiable functions reflecting the prey and predator growth rates, respectively. Therefore, we can solve (5) using the positive conditions $(N(0), P(0))$ to obtain:

$$N(T) = N(0)\, e^{\int_0^t \left[r_1\left(m+\frac{n(1-m)}{n+P(s)}\right)-d_1-bN(s)-\frac{(a+hP(s))P(s)}{c_1+(a+hP(s))N(s)+c_2P(s)}-q_1EN(s)\right]ds}$$

$$P(T) = P(0)e^{\int_0^t \left[r_2\left(1-\frac{P(s)}{K+(a+hP(s))N(s)}\right)-d_2N(s)-q_2EP(s)\right]ds}$$

As a result, of the exponential function's definition, any solution in the $int.\mathbb{R}_+^2 = \{(N,P) \in \mathbb{R}^2 : N(T) > 0, P(T) > 0\}$ that begins with positive starting conditions $(N(0), P(0))$ remains there eternally, due to the previous two equations.

Theorem 2. In the region,

$$\Upsilon = \left\{(N,P) \in \mathbb{R}_+^2 : 0 \le N < \frac{r_1 - d_1}{b + q_1 E}, 0 \le P < \frac{r_2}{q_2 E}\right\}.$$

All of the solutions to system (5) are uniformly bounded, where $r_1, r_2, d_1,\ q_1,\ q_2,\ E$, and b are positive constants that satisfy $r_1 - d_1 > 0$, which reflects the prey species' survival condition in the absence of the predator.

Proof. From the first equation of System (5), it is obtained that

$$\frac{dN}{dT} \le (r_1 - d_1)N - (b + q_1 E)N^2.$$

By solving the above differential inequality it is obtained that:

$$N(T) \le \frac{r_1 - d_1}{(b + q_1 E)[1 - e^{-(r_1 - d_1)T}] + (r_1 - d_1)N(0)e^{-(r_1 - d_1)T}}$$

Thus, if $T \to \infty$, it is obtained that $N(T) \le \frac{r_1 - d_1}{b + q_1 E} = \epsilon > 0$, because the survivor species' reproduction rate is naturally bigger than its mortality rate. Now from the subsequent equation of system (5), it is inferred that:

$$\frac{dP}{dT} \le r_2 P - q_2 E P^2$$

Similarly, solving the last differential inequality gives:

$$P(T) \le \frac{r_2}{q_2 E[1 - e^{-r_2 T}] + r_2 N(0) e^{-r_2 T}}.$$

Therefore, when $T \to \infty$, it is obtained that $P(T) \le \frac{r_2}{q_2 E}$. Consequently, the total solution of system (5) will be a uniformly bounded solution, hence the proof is complete.

3. POINTS OF EQUILIBRIUM AND THEIR STABILITY

The system (5) has four nonnegative equilibrium points. The entire extinction equilibrium point $s_0 = (0,0)$ always exists. The predator-free equilibrium point $s_1 = (\overline{N}, 0) = \left(\frac{r_1 - d_1}{b + q_1 E}, 0\right)$ that exists when $r_1 - d_1 > 0$. However, the prey-free equilibrium point $s_2 = \left(0, \overline{\overline{P}}\right) = \left(0, \frac{r_2 K}{r_2 + K q_2 E}\right)$ that always exists. Finally, the co-existing equilibrium point $e_3 = \left(\widehat{N}, \widehat{P}\right)$ is the intersection of the non-trivial prey and predator nullclines $f(N,P) = 0$ and $g(N,P) = 0$, where $f(N,P)$ and $g(N,P)$ are given in system (5).

Straightforward computation shows that these two nullclines intersect uniquely at e_3 in the region Υ if and only if the following set of sufficient conditions is met, see Figure (1a) using a selected set of data.

$$\left.\begin{array}{r}\frac{r_2}{d_2} < \frac{r_1-d_1}{b+q_1E}\\ \frac{dP}{dN} = -\frac{\partial f/\partial N}{\partial f/\partial P} < 0\\ \frac{dP}{dN} = -\frac{\partial g/\partial N}{\partial g/\partial P} > 0\end{array}\right\} \tag{6}$$

Now the Jacobian matrix of system (5) at the point (N, P) can be written as:

$$J = \left(a_{ij}\right)_{2\times 2}, \tag{7}$$

where

$$a_{11} = -\frac{2bN^3(a+hP)^2+(c_1+c_2P)\left(4bN^2+P\right)(a+hP)+2bN(c_1+c_2P)}{(c_1+N(a+hP)+c_2P)^2} - d_1 - 2Eq_1N + \frac{(n+mP)r_1}{n+P},$$

$$a_{12} = -\frac{N\left[N(a+hP)^2+c_1(a+2hP)+c_2hP^2\right]}{(c_1+(a+hP)N+c_2P)^2} - \frac{r_1(1-m)nN}{(n+P)^2},$$

$$a_{21} = P\left(-d_2 + \frac{r_2(a+hP)P}{(k+N(a+hP))^2}\right),$$

$$a_{22} = -d_2N - 2Eq_2P + r_2\left(1 - \frac{(2k+2aN+hNP)P}{(k+N(a+hP))^2}\right).$$

Therefore, the Jacobian matrix at the entire extinction point s_0 becomes:

$$J(s_0) = \begin{pmatrix} -d_1 + r_1 & 0 \\ 0 & r_2 \end{pmatrix}. \tag{8}$$

Consequently, the eigenvalues are given by

$$\lambda_{01} = -d_1 + r_1,\ \lambda_{02} = r_2. \tag{9}$$

Obviously, s_0 is a saddle point if the following condition is satisfied:

$$r_1 < d_1. \tag{10}$$

While it is an unstable node when

$$r_1 > d_1. \tag{11}$$

The Jacobian matrix (7) at predator-free equilibrium point s_1 becomes

$$J(s_1) = \left(\delta_{ij}\right)_{2\times 2}, \tag{12}$$

where

$$\delta_{11} = (r_1 - d_1)\left(1 - \frac{2Eq_1}{b+Eq_1} - \frac{2a^2b(r_1-d_1)^2+2bc_1(b+Eq_1)[c_1(b+Eq_1)+2a(r_1-d_1)]}{(b+Eq_1)[c_1(b+Eq_1)+a(r_1-d_1)]^2}\right).$$

$$\delta_{12} = -(r_1 - d_1)\left(\frac{(1-m)r_1}{n(b+eq_1)} + \frac{a}{c_1(b+eq_1)+\mathrm{a}(r_1-d_1)}\right).$$

$\delta_{21} = 0.$

$\delta_{22} = -\frac{d_2(r_1-d_1)}{b+Eq_1} + r_2.$

Hence the eigenvalues are given by:

$$\lambda_{11} = \delta_{11},\ \lambda_{12} = \delta_{22}. \tag{13}$$

Therefore, the equilibrium point s_1 is a stable node if and only if the following conditions hold.

$$1 < \frac{2Eq_1}{b+Eq_1} + \frac{2a^2b(r_1-d_1)^2+2bc_1(b+Eq_1)[c_1(b+Eq_1)+2a(r_1-d_1)]}{(b+Eq_1)[c_1(b+Eq_1)+a(r_1-d_1)]^2}. \tag{14}$$

$$r_2 < \frac{d_2(r_1-d_1)}{b+Eq_1}. \tag{15}$$

It is a saddle point if only one condition of the conditions (14)-(15) holds, while it is an unstable node when both conditions (14)-(15) are reflected. It is a non-hyperbolic point when one condition of (14)-(15) holds while equality occurs at the other condition.

The Jacobian matrix (7) at prey-free equilibrium point s_2 turns into:

$$J(s_2) = \left(b_{ij}\right)_{2\times 2}, \tag{16}$$

where

$b_{11} = -d_1 + \frac{r_1[n(Ekq_2+r_2)+kmr_2]}{n(Ekq_2+r_2)+kr_2} - \frac{kr_2[a(Ekq_2+r_2)+hkr_2]}{(Ekq_2+r_2)[c_1(Ekq_2+r_2)+kc_2r_2]},$

$b_{12} = 0,$

$b_{21} = \frac{r_2(-d_2k(Ekq_2+r_2)^2+r_2^2[a(Ekq_2+r_2)+hkr_2])}{(Ekq_2+r_2)^3},$

$b_{22} - r_2.$

Therefore, the eigenvalues can be written as:

$$\left.\begin{array}{c} \lambda_{21} = -d_1 + \frac{r_1[n(Ekq_2+r_2)+kmr_2]}{n(Ekq_2+r_2)+kr_2} - \frac{kr_2[a(Ekq_2+r_2)+hkr_2]}{(Ekq_2+r_2)[c_1(Ekq_2+r_2)+kc_2r_2]} \\ \lambda_{22} = -r_2 \end{array}\right\}. \tag{17}$$

Direct computation shows that, the equilibrium point s_2 is a stable node if the following condition is met.

$$\frac{r_1[n(Ekq_2+r_2)+kmr_2]}{n(Ekq_2+r_2)+kr_2} < d_1 + \frac{kr_2[a(Ekq_2+r_2)+hkr_2]}{(Ekq_2+r_2)[c_1(Ekq_2+r_2)+kc_2r_2]} \tag{18}$$

It is a saddle point if condition (18) is reflected, while it becomes a non-hyperbolic point when equality occurs.

Finally, the Jacobian matrix (7) at the co-existing point s_3 turns into

$$J = \left(\hat{a}_{ij}\right)_{2\times 2}, \tag{19}$$

where $\hat{a}_{ij} = a_{ij}(\hat{N}, \hat{P})$ for all $i.j = 1,2$.

Theorem 3. The co-existing point s_3 is a sink if and only if the following sufficient conditions are satisfied.

$$\frac{(n+m\hat{P})r_1}{n+\hat{P}} < \frac{2b\hat{N}^3(a+h\hat{P})^2+(c_1+c_2\hat{P})(4b\hat{N}^2+\hat{P})(a+h\hat{P})+2b\hat{N}(c_1+c_2\hat{P})}{(c_1+\hat{N}(a+h\hat{P})+c_2\hat{P})^2} + d_1 + 2Eq_1\hat{N}, \tag{20}$$

$$d_2 < \frac{r_2(a+h\hat{P})\hat{P}}{(k+\hat{N}(a+h\hat{P}))^2}, \tag{21}$$

$$r_2\left(1 - \frac{(2k+2a\hat{N}+h\hat{N}\hat{P})\hat{P}}{\left(k+\hat{N}(a+h\hat{P})\right)^2}\right) < d_2\hat{N} + 2Eq_2\hat{P}. \tag{22}$$

Proof. The characteristic polynomial of the Jacobian matrix (19) can be written in the form

$$\lambda^2 - T_r\lambda + D_e = 0, \tag{23}$$

where $T_r = \hat{a}_{11} + \hat{a}_{22}$ and $D_e = \hat{a}_{11}\hat{a}_{22} - \hat{a}_{12}\hat{a}_{21}$. According to Routh-Hurwitz criterion, the equation (23) have two roots with negative real parts if and only if $T_r < 0$, and $D_e > 0$. Direct calculations indicate that the above conditions (20)-(22) satisfy the requirements of the Routh-Hurwitz criterion. Therefore, the co-existing point is a sink.

Theorem 4. System (5) has no periodic solutions provided that the following sufficient condition holds

$$\frac{(a+hP)^2P}{(c_1+(a+hP)N+c_2P)^2} \leq b + q_1E. \tag{24}$$

Proof. Consider the continuously differentiable function $D(N,P) = \frac{1}{NP} > 0$, for all (N,P) belongs to the first quadrant $int.\mathbb{R}_+^2$.

Therefore, direct computation gives the following expression

$$\Delta = \frac{\partial}{\partial N}\left(D\frac{dN}{dT}\right) + \frac{\partial}{\partial P}\left(D\frac{dP}{dT}\right) = -\frac{b}{P} + \frac{(a+hP)^2}{(c_1+(a+hP)N+c_2P)^2} - \frac{q_1E}{P} - \frac{r_2}{N}\frac{K+aN}{(K+(a+hP)N)^2} - \frac{q_2E}{N}$$

Clearly, $\Delta < 0$ provided that condition (24) holds. Therefore, according to the Bendixson–Dulac theorem [39], there are nonconstant periodic solutions in the first quadrant of the system (5) provided that condition (24) holds.

As a result of theorem (4), using the Poincare-Bendixson theorem, the unique co-existing equilibrium point of the system (5) in the interior of the first quadrant is a globally asymptotically stable point.

4. Uniformly Persistence

Mathematically, uniform persistence refers to the presence of an area in the phase plane at a positive distance from the border where population species arrive and must eventually lie, guaranteeing the ongoing existence of species in a biological sense. Uniform persistence is defined analytically as follows.

Definition [40]: The system (5) is uniformly persistent if every solution $(N(T), P(T))$ of it given that the initial condition $\big(N(0), P(0)\big) \in int.\mathbb{R}_+^2$ fulfills the following requirements:

(i) $N(T) > 0,\ P(T) > 0$ for all T >0.

(ii) There exists $\epsilon > 0$ so that $\lim_{T\to\infty}\inf N(T) > \epsilon$ and $\lim_{T\to\infty}\inf P(T) > \epsilon$.

Theorem 5. The system (5) is uniformly persistent provided that

$$d_1(nq_2E + r_2) < m(nq_2E + r_2) + n(1-m)q_2E. \tag{25}$$

Proof. From the first equation of system (1), for $T > T_1$ it is obtained

$$\begin{aligned}\frac{dN}{dT} &= N\left[r_1\left(m + \frac{n(1-m)}{n+P}\right) - d_1 - bN - \frac{(a+hP)P}{c_1+(a+hP)N+c_2P} - q_1EN\right] \\ &\geq N\left[r_1\left(\frac{m(nq_2E+r_2)+n(1-m)q_2E-d_1(nq_2E+r_2)}{nq_2E+r_2}\right) - (b+q_1E)N\right]\end{aligned}$$

Therefore, due to lemma (2.2) of [40], the following is obtained.

$$\lim_{T\to\infty}\inf N(T) \geq \frac{m(nq_2E+r_2)+n(1-m)q_2E-d_1(nq_2E+r_2)}{(nq_2E+r_2)(b+q_1E)} \equiv \sigma_1$$

Similarly, from the second equation of system (5), it is observed that

$$\frac{dP}{dT} = P\left[r_2\left(1 - \frac{P}{K+(a+hP)N}\right) - d_2\mathrm{N} - q_2EP\right] \geq P\left[r_2 - \frac{(r_2+Kq_2E)}{K}P\right].$$

Again, using lemma (2.2) of [40], the following is obtained

$$\lim_{T\to\infty}\inf P(T) \geq \frac{r_2K}{(r_2+Kq_2E)} \equiv \sigma_2.$$

Thus, for arbitrary $\epsilon > 0$, so that $\epsilon = \min\{\sigma_1, \sigma_2\}$, it is obtained that

$$\lim_{T\to\infty}\inf N(T) > \epsilon \text{ and } \lim_{T\to\infty}\inf P(T) > \epsilon$$

The proof is done.

5. LOCAL BIFURCATION

Changes in the qualitative structure of a collection of curves, such as the integral curves of a set of vector fields or the solutions of a set of differential equations, are investigated by bifurcation theory. A bifurcation happens when a slight smooth change in the parameter values of a system results in a major significant shift in its behavior. It is most frequently employed in the mathematical analysis of dynamical systems. Bifurcation might take place in two ways. Local bifurcations are visible when parameters pass through vital thresholds by observing alterations in the regional stability features of equilibria, periodic orbits, or other invariant sets; global bifurcations take place when the system's larger consistent sets clash with each other or with the system's equilibria. They cannot be discovered just by looking at the stability of the equilibria. The identification of the probability of local bifurcation is worked out in this part. Consider the system (5) in the form

$$\frac{d\mathbf{Y}}{dT}=\mathbf{F}(\mathbf{Y}),\text{ with } \mathbf{Y}=\begin{pmatrix}N\\P\end{pmatrix},\text{ and } \mathbf{F}=\begin{pmatrix}f_1(N,P,\mu)\\g_1(N,P,\mu)\end{pmatrix}=\begin{pmatrix}Nf(N,P,\mu)\\Pg(N,P,\mu)\end{pmatrix}. \tag{26}$$

where $\mu\in\mathbb{R}$ be the parameter.

Consequently, the second directional derivative of $\mathbf{F}$, where $\mathbf{V}=(v_1,v_2)^T$ be any vector, can be written using direct computation as:

$$D^2\mathbf{F}(\mathbf{Y},\mu).(\mathbf{V},\mathbf{V})=\begin{pmatrix}c_{11}\\c_{21}\end{pmatrix}, \tag{27}$$

where

$$\begin{aligned}c_{11}&=2\left(-b-\frac{(a+hP)^3NP}{(c_1+N(a+hP)+c_2P)^3}+\frac{(a+hP)^2P}{(c_1+N(a+hP)+c_2P)^2}-Eq_1\right)v_1^2\\&\quad+2\left[\left(\frac{c_1[-aN(a+hP)-c_1(a+2hP)]-c_2P[N(a+hP)(2a+hP)+c_1(a+3hP)]-c_2^2hP^3}{(c_1+N(a+hP)+c_2P)}\right)\right.\\&\qquad\left.-\frac{(1-m)nr_1}{(n+P)^2}\right]v_1v_2+2N\left(\frac{(aN+c_1)(-hc_1+ac_2)}{(c_1+N(a+hP)+c_2P)^3}+\frac{(1-m)nr_1}{(n+P)^3}\right)v_2^2\\c_{21}&=-\frac{2r_2P^2(a+hP)^2}{\left(k+N(a+hP)\right)^3}v_1^2-2\left[Eq_2+\frac{r_2(k+aN)^2}{\left(k+N(a+hP)\right)^3}\right]v_2^2\\&\quad-2\left[d_2-\frac{r_2P[2a(k+aN)+3h(k+aN)P+h^2NP^2]}{\left(k+N(a+hP)\right)^3}\right]v_1v_2\end{aligned}$$

Theorem 6. At $r_2=\frac{d_2(r_1-d_1)}{b+Eq_1}\equiv r_2^*$, the system (5) enters into transcritical bifurcation around the predator-free equilibrium point provided that condition (14) holds along with the following condition

$$2d_2\frac{\bar{\delta}_{12}^*}{\bar{\delta}_{11}^*} \neq 2\left[hq_2 + \frac{r_2}{(k+a\bar{N})}\right]. \tag{28}$$

Otherwise, the system (5) enters into pitchfork bifurcation provided that the following condition is met.

$$\frac{6r_2h\bar{N}}{(k+a\bar{N})^2} \neq \frac{6r_2a}{(k+a\bar{N})^2}\frac{\bar{\delta}_{12}^*}{\bar{\delta}_{11}^*}. \tag{29}$$

Proof. From the Jacobian matrix (12) at $r_2 = r_2^*$, it is obtained that

$$J_1 = J(s_1, r_2^*) = \left(\bar{\delta}_{ij}^*\right)_{2\times 2},$$

Where $\bar{\delta}_{ij}^* = \delta_{ij}(s_1, r_2^*)$, with δ_{ij} given in equation (12) and $\bar{\delta}_{22}^* = \delta_{22}(s_1, r_2^*) = 0$. Therefore, The eigenvalues of J_1 are given by $\lambda_{11}{}^* = \bar{\delta}_{11}^* < 0$ due to condition (14), and $\lambda_{12}{}^* = 0$. Hence, s_1 is a non-hyperbolic point. Let $\mathbf{V_1} = \begin{pmatrix} v_{11} \\ v_{21} \end{pmatrix}$, and $\mathbf{U_1} = \begin{pmatrix} u_{11} \\ u_{21} \end{pmatrix}$ reperesent the eigenvectors corresponding to the $\lambda_{12}{}^* = 0$ of the J_1 and their transpose respectively. Then, straightforward computation gives that:

$$\mathbf{V_1} = \begin{pmatrix} -\frac{\bar{\delta}_{12}^*}{\bar{\delta}_{11}^*} \\ 1 \end{pmatrix} \equiv \begin{pmatrix} \pi_1 \\ 1 \end{pmatrix}, \text{ and } \mathbf{U_1} = \begin{pmatrix} 0 \\ 1 \end{pmatrix}.$$

Obviously, $\pi_1 < 0$ due to $\bar{\delta}_{12}^* < 0$ and $\bar{\delta}_{11}^* < 0$ from condition (14). Moreover, direct computation shows that:

$$\mathbf{F}_{r_2}(\mathbf{Y}, r_2) = \begin{pmatrix} 0 \\ \left(1 - \frac{P}{K+(a+hP)N}\right)P \end{pmatrix} \Rightarrow \mathbf{F}_{r_2}(s_1, r_2^*) = \begin{pmatrix} 0 \\ 0 \end{pmatrix}.$$

Hence, it is obtained that $\Delta_{11} = \mathbf{U_1}^{\mathrm{T}}\mathbf{F}_{r_2}(s_1, r_2^*) = 0$. Moreover, it is observed that

$$\Delta_{21} = \mathbf{U_1}^{\mathrm{T}}\left[D\mathbf{F}_{r_2}(s_1, r_2^*)\mathbf{V_1}\right] = 1 \neq 0.$$

Furthermore, according to the equation (27), it is obtained that

$$D^2\mathbf{F}_{r_2}(s_1, r_2^*)(\mathbf{V_1}, \mathbf{V_1}) = \begin{pmatrix} \bar{c}_{11} \\ \bar{c}_{21} \end{pmatrix},$$

where

$$\bar{c}_{11} = -2(b + Eq_1)\pi_1^2 - 2\left[c_1a + \frac{(1-m)r_1}{n}\right]\pi_1 + 2\bar{N}\left(\frac{(-hc_1 + ac_2)}{(a\bar{N} + c_1)^2} + \frac{(1-m)r_1}{n^2}\right).$$

$$\bar{c}_{21} = -2\left[Eq_2 + \frac{r_2}{(k+a\bar{N})}\right] - 2d_2\pi_1.$$

Hence,

$$\Delta_{31} = \mathbf{U_1}^{\mathrm{T}}\left[D^2\mathbf{F}_{r_2}(s_1, r_2^*)(\mathbf{V_1}, \mathbf{V_1})\right] = -2\left[Eq_2 + \frac{r_2}{(k+a\bar{N})}\right] - 2d_2\pi_1$$
$$= -2\left[hq_2 + \frac{r_2}{(k+a\bar{N})}\right] + 2d_2\frac{\bar{\delta}_{12}^*}{\bar{\delta}_{11}^*}.$$

Consequently, $\Delta_{31} \neq 0$ provided that condition (28) is satisfied. Hence from the values of Δ_{11}, Δ_{21}, and Δ_{31}, Sotomayor theorem of local bifurcation leads to the fact that system (5) enters into transcritical bifurcation around the predator-free equilibrium point.

However, if the condition (28) is violated then direct computation to the third directional derivative of $\mathbf{F}$ at (s_1, r_2^*) gives that

$$D^3\mathbf{F}_{r_2}(s_1, r_2^*)(\mathbf{V_1}, \mathbf{V_1}, \mathbf{V_1}) = \begin{pmatrix} \bar{l}_{11} \\ \bar{l}_{21} \end{pmatrix}$$

where

$$\begin{aligned}\bar{l}_{11} = -\frac{6}{n^4(a\bar{N}+c_1)^4}[(&-ah^2n^4\bar{N}^3c_1 - h^2n^4\bar{N}^2c_1^2 + a^2hn^4\bar{N}^3c_2 - hn^4\bar{N}c_1^2c_2 \\ &+a^2n^4\bar{N}^2c_2^2 + an^4\bar{N}c_1c_2^2 + a^4n\bar{N}^5r_1 - a^4mn\bar{N}^5r_1 + 4a^3n\bar{N}^4c_1r_1 \\ &-4a^3mn\bar{N}^4c_1r_1 + 6a^2n\bar{N}^3c_1^2r_1 - 6a^2mn\bar{N}^3c_1^2r_1 + 4an\bar{N}^2c_1^3r_1 - 4amn\bar{N}^2c_1^3r_1 \\ &+n\bar{N}c_1^4r_1 - mn\bar{N}c_1^4r_1) + (-a^2hn^4\bar{N}^2c_1 + hn^4c_1^3 + a^3n^4\bar{N}^2c_2 - an^4c_1^2c_2 \\ &-a^4n^2\bar{N}^4r_1 + a^4mn^2\bar{N}^4r_1 - 4a^3n^2\bar{N}^3c_1r_1 + 4a^3mn^2\bar{N}^3c_1r_1 - 6a^2n^2\bar{N}^2c_1^2r_1 \\ &+6a^2mn^2\bar{N}^2c_1^2r_1 - 4an^2\bar{N}c_1^3r_1 + 4amn^2\bar{N}c_1^3r_1 - n^2c_1^4r_1 + mn^2c_1^4r_1)\pi_1 \\ &+(-a^3n^4\bar{N}c_1 - a^2n^4c_1^2)\pi_1^2]\end{aligned}.$$

$$\bar{l}_{21} = \frac{6r_2(h\bar{N}+a\pi_1)}{(k+a\bar{N})^2}.$$

Hence,

$$\Delta_{41} = \mathbf{U_1}^{\mathrm{T}}\left[D^3\mathbf{F}_{r_2}(s_1, r_2^*)(\mathbf{V_1}, \mathbf{V_1}, \mathbf{V_1})\right] = \frac{6r_2(h\bar{N}+a\pi_1)}{(k+a\bar{N})^2} = \frac{6r_2h\bar{N}}{(k+a\bar{N})^2} - \frac{6r_2a}{(k+a\bar{N})^2}\frac{\bar{\delta}_{12}^*}{\bar{\delta}_{11}^*}$$

Therefore, $\Delta_{41} \neq 0$ provided that condition (29) is satisfied. Thus from the values of Δ_{11}, Δ_{21}, Δ_{31}, and Δ_{41}, the Sotomayor theorem of local bifurcation leads to the fact that system (5) enters into pitchfork bifurcation around the predator-free equilibrium point and that completes the proof.

Theorem 7. At $d_1 = \frac{r_1[n(Ekq_2+r_2)+kmr_2]}{n(Ekq_2+r_2)+kr_2} - \frac{kr_2[a(Ekq_2+r_2)+hkr_2]}{(Ekq_2+r_2)[c_1(Ekq_2+r_2)+kc_2r_2]} \equiv d_1^*$, then the system (5) enters into a transcritical bifurcation around the prey-free equilibrium point provided that

$$\bar{\bar{c}}_{11} \neq 0. \tag{30}$$

Otherwise, the system (5) enters into pitchfork bifurcation provided that the following condition is met.

$$\bar{\bar{l}}_{11} \neq 0. \tag{31}$$

Where all the new symbols are given in the proof.

Proof. From the Jacobian matrix (15) at $d_1 = d_1^*$, it is obtained that

$$J_2 = J(s_2, d_1^*) = \left(b_{ij}^*\right)_{2\times 2}.$$

where $b_{ij}^* = b_{ij}(d_1^*)$ with b_{ij} are given in equation (15) and $b_{11}^* = b_{11}(d_1^*) = 0$.

Therefore, the eigenvalues of J_2 are given by $\lambda_{21}{}^* = 0$ under the condition (17), and $\lambda_{22}{}^* = -r_2$. Hence, s_2 is a non-hyperbolic point. Let $\mathbf{V_2} = \begin{pmatrix} v_{12} \\ v_{22} \end{pmatrix}$, and $\mathbf{U_2} = \begin{pmatrix} u_{12} \\ u_{22} \end{pmatrix}$ denotes to the eigenvectors corresponding to the $\lambda_{11}{}^* = 0$ of the J_2 and their transpose respectively. Then, straightforward computation gives that:

$$\mathbf{V_2} = \begin{pmatrix} 1 \\ -\frac{b_{21}^*}{b_{22}^*} \end{pmatrix} = \begin{pmatrix} 1 \\ \pi_2 \end{pmatrix}, \text{ and } \mathbf{U_2} = \begin{pmatrix} 1 \\ 0 \end{pmatrix}.$$

Moreover, direct computation shows that:

$$\mathbf{F}_{d_1}(\mathbf{Y}, d_1) = \begin{pmatrix} -\mathrm{N} \\ 0 \end{pmatrix} \Rightarrow \mathbf{F}_{d_1}(s_2, d_1^*) = \begin{pmatrix} 0 \\ 0 \end{pmatrix}.$$

Hence, it is obtained that $\Delta_{12} = \mathbf{U_2}^{\mathrm{T}} \mathbf{F}_{d_1}(s_2, d_1^*) = 0$. Also, it is observed that

$$\Delta_{22} = \mathbf{U_2}^{\mathrm{T}}\left[D\mathbf{F}_{d_1}(s_2, d_1^*)\mathbf{V_2}\right] = -1 \neq 0.$$

Furthermore, according to the equation (27), it is obtained that

$$D^2\mathbf{F}_{d_1}(s_2, d_1^*)(\mathbf{V_2}, \mathbf{V_2}) = \begin{pmatrix} \bar{\bar{c}}_{11} \\ \bar{\bar{c}}_{21} \end{pmatrix},$$

where

$$\bar{\bar{c}}_{11} = 2\left(-b + \frac{(a+hP)^2 P}{(c_1+c_2P)^2} - Eq_1\right) - 2\left[\frac{c_1{}^2(a+2hP)+c_2c_1(a+3hP)P+c_2^2hP^3}{(c_1+c_2P)} + \frac{(1-m)nr_1}{(n+P)^2}\right]\pi_2.$$

$$\bar{\bar{c}}_{21} = -\frac{2r_2P^2(a+hP)^2}{k^3} - 2\left[Eq_2 + \frac{r_2}{k}\right]\pi_2{}^2 - 2\left[d_2 - \frac{r_2P[2a+3hP]}{k^2}\right]\pi_2.$$

Hence, $\Delta_{32} = \mathbf{U_2}^{\mathrm{T}}\left[D^2\mathbf{F}_{d_1}(s_2, d_1^*)(\mathbf{V_2}, \mathbf{V_2})\right] = \bar{\bar{c}}_{11}$.

Consequently, $\Delta_{32} \neq 0$ provided that condition (30) is satisfied. Hence from the values of Δ_{12}, Δ_{22}, and Δ_{32}, Sotomayor theorem of local bifurcation leads to the fact that system (5) enters into transcritical bifurcation around the prey-free equilibrium point.

On the other hand, if the condition (29) is violated then direct computation to the third directional derivative of $\mathbf{F}$ at (s_2, d_1^*) gives that

$$D^3\mathbf{F}_{d_1}(s_2, d_1^*)(\mathbf{V_2}, \mathbf{V_2}, \mathbf{V_2}) = \begin{pmatrix} \bar{\bar{l}}_{11} \\ \bar{\bar{l}}_{21} \end{pmatrix},$$

where

$$\bar{\bar{l}}_{11} = -\frac{6[H_1 + H_2\pi_2 + H_3\pi_2^2]}{(n+\bar{\bar{P}})^4(c_1+c_2\bar{\bar{P}})^4},$$

$$\bar{\bar{l}}_{21} = \frac{6(a^3\bar{\bar{P}}^2 + 3a^2h\bar{\bar{P}}^3 + 3ah^2\bar{\bar{P}}^4 + h^3\bar{\bar{P}}^5)r_2}{k^4} - \frac{6(2a^2k\bar{\bar{P}} + 6ahk\bar{\bar{P}}^2 + 4h^2k\bar{\bar{P}}^3)r_2\pi_2}{k^4} + \frac{6(ak^2 + 3hk^2\bar{\bar{P}})r_2\pi_2^2}{k^4},$$

where

$$\begin{aligned} H_1 &= a^3n^4c_1\bar{\bar{P}} + 4a^3n^3\bar{\bar{P}}^2c_1 + 3a^2hn^4\bar{\bar{P}}^2c_1 + 6a^3n^2\bar{\bar{P}}^3c_1 + 12a^2hn^3\bar{\bar{P}}^3c_1 + 3ah^2n^4\bar{\bar{P}}^3c_1 \\ &+4a^3n\bar{\bar{P}}^4c_1 + 18a^2hn^2\bar{\bar{P}}^4c_1 + 12ah^2n^3\bar{\bar{P}}^4c_1 + h^3n^4\bar{\bar{P}}^4c_1 + a^3\bar{\bar{P}}^5c_1 + 12a^2hn\bar{\bar{P}}^5c_1 \\ &+18ah^2n^2\bar{\bar{P}}^5c_1 + 4h^3n^3\bar{\bar{P}}^5c_1 + 3a^2h\bar{\bar{P}}^6c_1 + 12ah^2n\bar{\bar{P}}^6c_1 + 6h^3n^2\bar{\bar{P}}^6c_1 + 3ah^2\bar{\bar{P}}^7c_1 \\ &+4h^3n\bar{\bar{P}}^7c_1 + h^3\bar{\bar{P}}^8c_1 + a^3n^4\bar{\bar{P}}^2c_2 + 4a^3n^3\bar{\bar{P}}^3c_2 + 3a^2hn^4\bar{\bar{P}}^3c_2 + 6a^3n^2\bar{\bar{P}}^4c_2 \\ &+12a^2hn^3\bar{\bar{P}}^4c_2 + 3ah^2n^4\bar{\bar{P}}^4c_2 + 4a^3n\bar{\bar{P}}^5c_2 + 18a^2hn^2\bar{\bar{P}}^5c_2 + 12ah^2n^3\bar{\bar{P}}^5c_2 \\ &+h^3n^4\bar{\bar{P}}^5c_2 + a^3\bar{\bar{P}}^6c_2 + 12a^2hn\bar{\bar{P}}^6c_2 + 18ah^2n^2\bar{\bar{P}}^6c_2 + 4h^3n^3\bar{\bar{P}}^6c_2 + 3a^2h\bar{\bar{P}}^7c_2 \\ &+12ah^2n\bar{\bar{P}}^7c_2 + 6h^3n^2\bar{\bar{P}}^7c_2 + 3ah^2\bar{\bar{P}}^8c_2 + 4h^3n\bar{\bar{P}}^8c_2 + h^3\bar{\bar{P}}^9c_2 \end{aligned}.$$

$$\begin{aligned} H_2 &= -a^2n^4c_1^2 - 4a^2n^3\bar{\bar{P}}c_1^2 - 4ahn^4\bar{\bar{P}}c_1^2 - 6a^2n^2\bar{\bar{P}}^2c_1^2 - 16ahn^3\bar{\bar{P}}^2c_1^2 - 3h^2n^4\bar{\bar{P}}^2c_1^2 \\ &-4a^2n\bar{\bar{P}}^3c_1^2 - 24ahn^2\bar{\bar{P}}^3c_1^2 - 12h^2n^3\bar{\bar{P}}^3c_1^2 - a^2\bar{\bar{P}}^4c_1^2 - 16ahn\bar{\bar{P}}^4c_1^2 \\ &-18h^2n^2\bar{\bar{P}}^4c_1^2 - 4ah\bar{\bar{P}}^5c_1^2 - 12h^2n\bar{\bar{P}}^5c_1^2 - 3h^2\bar{\bar{P}}^6c_1^2 - 4ahn^4\bar{\bar{P}}^2c_1c_2 \\ &-16ahn^3\bar{\bar{P}}^3c_1c_2 - 4h^2n^4\bar{\bar{P}}^3c_1c_2 - 24ahn^2\bar{\bar{P}}^4c_1c_2 - 16h^2n^3\bar{\bar{P}}^4c_1c_2 \\ &-16ahn\bar{\bar{P}}^5c_1c_2 - 24h^2n^2\bar{\bar{P}}^5c_1c_2 - 4ah\bar{\bar{P}}^6c_1c_2 - 16h^2n\bar{\bar{P}}^6c_1c_2 - 4h^2\bar{\bar{P}}^7c_1c_2 \\ &+a^2n^4\bar{\bar{P}}^2c_2^2 + 4a^2n^3\bar{\bar{P}}^3c_2^2 + 6a^2n^2\bar{\bar{P}}^4c_2^2 - h^2n^4\bar{\bar{P}}^4c_2^2 + 4a^2n\bar{\bar{P}}^5c_2^2 \\ &-4h^2n^3\bar{\bar{P}}^5c_2^2 + a^2\bar{\bar{P}}^6c_2^2 - 6h^2n^2\bar{\bar{P}}^6c_2^2 - 4h^2n\bar{\bar{P}}^7c_2^2 - h^2\bar{\bar{P}}^8c_2^2 \end{aligned}.$$

$$\begin{aligned} H_3 &= hn^4c_1^3 + 4hn^3\bar{\bar{P}}c_1^3 + 6hn^2\bar{\bar{P}}^2c_1^3 + 4hn\bar{\bar{P}}^3c_1^3 + h\bar{\bar{P}}^4c_1^3 - an^4c_1^2c_2 - 4an^3\bar{\bar{P}}c_1^2c_2 \\ &+hn^4\bar{\bar{P}}c_1^2c_2 - 6an^2\bar{\bar{P}}^2c_1^2c_2 + 4hn^3\bar{\bar{P}}^2c_1^2c_2 - 4an\bar{\bar{P}}^3c_1^2c_2 + 6hn^2\bar{\bar{P}}^3c_1^2c_2 \\ &-a\bar{\bar{P}}^4c_1^2c_2 + 4hn\bar{\bar{P}}^4c_1^2c_2 + h\bar{\bar{P}}^5c_1^2c_2 - an^4\bar{\bar{P}}c_1c_2^2 - 4an^3\bar{\bar{P}}^2c_1c_2^2 - 6an^2\bar{\bar{P}}^3c_1c_2^2 \\ &-4an\bar{\bar{P}}^4c_1c_2^2 - a\bar{\bar{P}}^5c_1c_2^2 - n^2c_1^4r_1 + mn^2c_1^4r_1 - n\bar{\bar{P}}c_1^4r_1 + mn\bar{\bar{P}}c_1^4r_1 \\ &-4n^2\bar{\bar{P}}c_1^3c_2r_1 + 4mn^2\bar{\bar{P}}c_1^3c_2r_1 - 4n\bar{\bar{P}}^2c_1^3c_2r_1 + 4mn\bar{\bar{P}}^2c_1^3c_2r_1 - 6n^2\bar{\bar{P}}^2c_1^2c_2^2r_1 \\ &+6mn^2\bar{\bar{P}}^2c_1^2c_2^2r_1 - 6n\bar{\bar{P}}^3c_1^2c_2^2r_1 + 6mn\bar{\bar{P}}^3c_1^2c_2^2r_1 - 4n^2\bar{\bar{P}}^3c_1c_2^3r_1 \\ &+4mn^2\bar{\bar{P}}^3c_1c_2^3r_1 - 4n\bar{\bar{P}}^4c_1c_2^3r_1 + 4mn\bar{\bar{P}}^4c_1c_2^3r_1 - n^2\bar{\bar{P}}^4c_2^4r_1 \\ &+mn^2\bar{\bar{P}}^4c_2^4r_1 - n\bar{\bar{P}}^5c_2^4r_1 + mn\bar{\bar{P}}^5c_2^4r_1 \end{aligned}.$$

Hence,

$$\Delta_{42} = \mathbf{U_2}^{\mathrm{T}}\left[D^3\mathbf{F}_{d_1}(s_2, d_1^*)(\mathbf{V_2}, \mathbf{V_2}, \mathbf{V_2})\right] = \bar{\bar{l}}_{11}$$

Therefore, $\Delta_{42} \neq 0$ provided that condition (31) is satisfied. Thus from the values of Δ_{12}, Δ_{22}, Δ_{32}, and Δ_{42}, Sotomayor theorem of local bifurcation leads to the fact that system (5) enters into pitchfork bifurcation around the prey-free equilibrium point and that completes the proof.

Theorem 8. Assume that condition (20) holds with $d_2 = d_2^*$, where

$$d_2^* = \frac{2Eq_2\hat{P}\hat{a}_{11}^* - r_2\left(1 - \frac{(2k+2a\hat{N}+h\hat{N}\hat{P})\hat{P}}{\left(k+\hat{N}(a+h\hat{P})\right)^2}\right)\hat{a}_{11}^* + \frac{r_2(a+h\hat{P})\hat{P}^2\hat{a}_{12}^*}{\left(k+\hat{N}(a+h\hat{P})\right)^2}}{(\hat{a}_{12}^*\hat{P} - \hat{N}\hat{a}_{11}^*)}.$$

Then the system (5) enters into a saddle-node bifurcation around the co-existing equilibrium point provided that

$$\hat{a}_{11}^* + \hat{a}_{22}^* < 0. \tag{32}$$

$$\pi_4\hat{c}_{11} + \hat{c}_{21} \neq 0. \tag{33}$$

Where all the new symbols are given in the proof.

Proof. From the Jacobian matrix (19) at $d_2 = d_2^*$, it is obtained that

$$J_3 = J(s_3, d_2^*) = \left(\hat{a}_{ij}^*\right).$$

where $\hat{a}_{ij}^* = \hat{a}_{ij}(d_2^*)$ and $\hat{a}_{ij}$ are given in equation (19).

Therefore, the determinant of J_3 that is given by $D_e(d_2^*)$ in equation (23) equals zero, that is $D_e(d_2^*) = 0$. So the characteristic equation (23) at $d_2 = d_2^*$ have eigenvalues $\lambda_1^* = 0$ and $\lambda_2^* = T_r(d_2^*) = \hat{a}_{11}^* + \hat{a}_{22}^* < 0$ under condition (32). Hence, s_3 is a non-hyperbolic point. Let $\mathbf{V_3} = \binom{v_{13}}{v_{23}}$, and $\mathbf{U_3} = \binom{u_{13}}{u_{23}}$ denote to the eigenvectors corresponding to the $\lambda_1^* = 0$ of the J_3 and their transpose respectively. Then, straightforward computation gives that:

$$\mathbf{V_3} = \begin{pmatrix} -\frac{\hat{a}_{12}^*}{\hat{a}_{11}^*} \\ 1 \end{pmatrix} = \binom{\pi_3}{1}, \text{ and } \mathbf{U_3} = \begin{pmatrix} -\frac{\hat{a}_{21}^*}{\hat{a}_{11}^*} \\ 1 \end{pmatrix} = \binom{\pi_4}{1}.$$

Moreover, direct computation shows that:

$$\mathbf{F}_{d_2}(\mathbf{Y}, d_2) = \binom{0}{-NP} \Rightarrow \mathbf{F}_{d_2}(s_3, d_2^*) = \binom{0}{-\hat{N}\hat{P}}.$$

Hence, it is obtained that $\Delta_{13} = \mathbf{U_3}^{\mathrm{T}}\mathbf{F}_{d_2}(s_3, d_2^*) = -\hat{N}\hat{P} \neq 0$.

Furthermore, according to the equation (27), it is obtained that

$$D^2\mathbf{F}_{d_2}(s_3, d_2^*)(\mathbf{V_3}, \mathbf{V_3}) = \begin{pmatrix} \hat{c}_{11} \\ \hat{c}_{21} \end{pmatrix},$$

where $\hat{c}_{11} = c_{11}(s_3, d_2^*)$ and $\hat{c}_{22} = c_{22}(s_3, d_2^*)$, with c_{11} and c_{22} are given in equation (27). Hence,

$$\Delta_{23} = \mathbf{U_3}^{\mathrm{T}}\left[D^2\mathbf{F}_{d_2}(s_3, d_2^*)(\mathbf{V_3}, \mathbf{V_3})\right] = \pi_4\hat{c}_{11} + \hat{c}_{21} .$$

Consequently, $\Delta_{23} \neq 0$ due to condition (33), so from the values of Δ_{13}, and Δ_{23}, Sotomayor theorem of local bifurcation leads to the fact that system (5) enters into a saddle-node bifurcation around the co-existing equilibrium point and that completes the proof.

6. SIMULATION ANALYSIS

It is well known that, the natural environment's interaction between prey and predator is one of mutual constraint and control. To further understand the dynamic connection between prey and predator, numerical simulations of the model (5) will be run to demonstrate some complicated dynamic behaviors. For simplicity, we set the parameters values as follows:

$$\begin{gathered} r_1 = 2, n = 2, m = 0.5, b = 0.1, d_1 = 0.1, a = 0.75, c_1 = 0.5, c_2 = 0.2 \\ h = 0.05, q_1 = 0.1, q_2 = 0.2, E = 0.75, r_2 = 1, K = 2, d_2 = 0.25. \end{gathered} \tag{34}$$

First, to demonstrate the existence of co-existing equilibrium point Figure (1) is given:

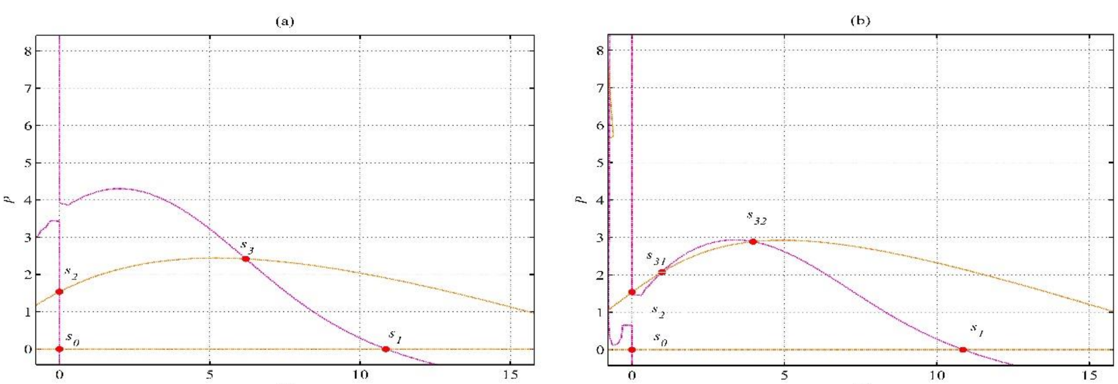

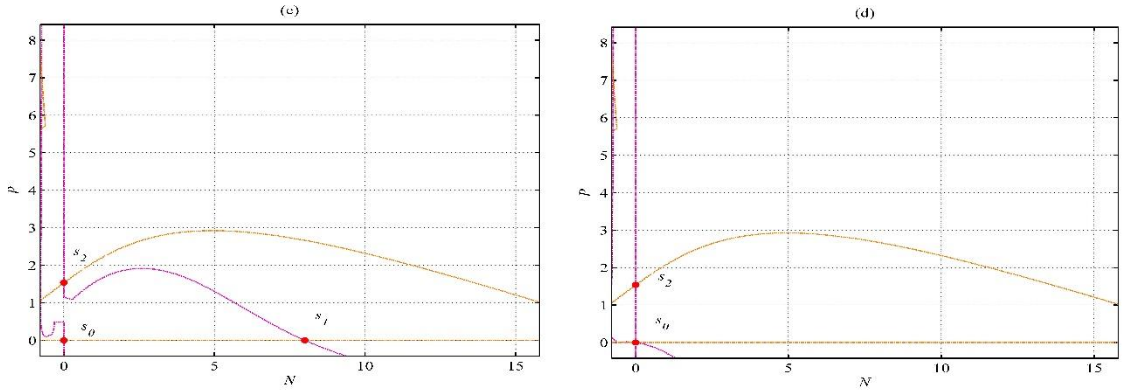

Fig. 1: Four conceivable cases for system's (5) nullclines. (a) Unique co-existing equilibrium point $s_3 = (6.2, 2.41)$ with $s_2 = (0, 1.53)$, $s_1 = (10.85, 0)$, and $s_0 = (0,0)$ for the data set (34) with $c_1 = 2$ and $d_2 = 0.05$. (b) Two co-existing equilibrium points $s_{31} = (0.98, 2.07)$ and $s_{32} = (3.97, 2.88)$ with three boundary points s_0, s_1, and s_2 for the data set (34). (c) Non existence of co-existing point for data set (34) with $r_1 = 1.5$. (d) Non existence of co-existing point and s_1 for the data set (34) with $r_1 = 0.1$.

Now, to understand the role of r_1 on the dynamics of the system (5), the numerical solution was obtained for different values of r_1. It is observed that for $r_1 \leq 0.1$ there are only two boundary points s_0 and $s_2 = (0, 1.53)$, which are source and sink (stable node) respectively. For, $0.1 < r_1 \leq 1.88$ the system has three boundary points s_0, s_1, and $s_2 = (0, 1.53)$, which are source, saddle, and sink respectively. However, for $1.88 < r_1 \leq 2.89$, system (5) has three boundary points s_0, s_1 and $s_2 = (0, 1.53)$ with two co-existing points s_{31} and s_{32} so that the system exhibits bistable case between s_2 and s_{32} while the rest of points are unstable. For $2.89 < r_1 \leq 3.63$, there is a unique co-existing point with three boundary points and the system exhibits bistable between s_2 and s_3 up to $r_1 = 3.13$ after that s_3 becomes a worldwide sink. Finally, for $r_1 > 3.63$ the system (5) has three boundary equilibrium point only s_0, s_1, and $s_2 = (0, 1.53)$ behave as source, worldwide sink, and saddle point. To explain the above-obtained results, Figure (2) is obtained using a numerical solution of the system (5) depending on parameters (34) with the selected values of r_1.

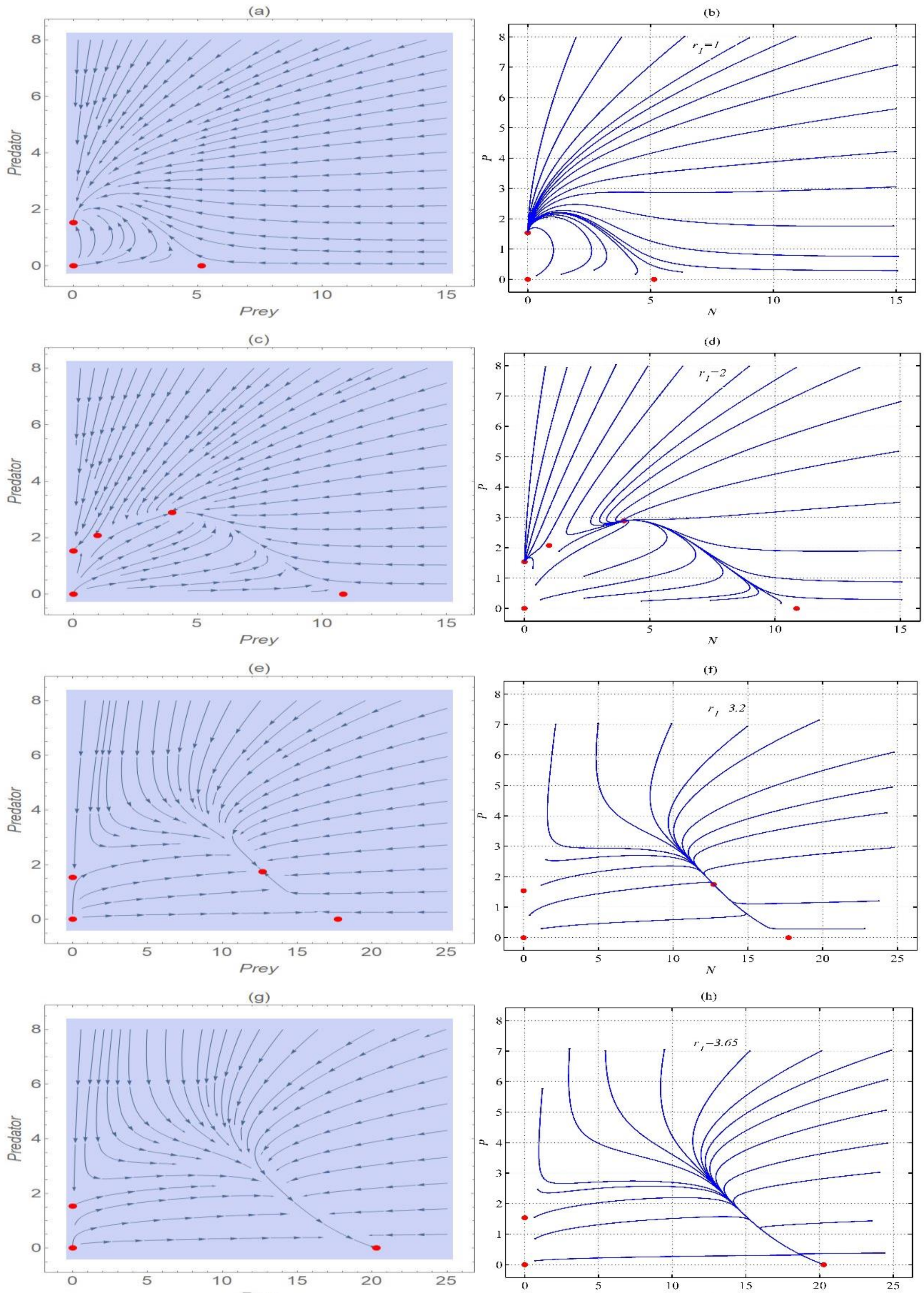

Fig. 2: (a) Direction field when $r_1 = 1$. (b) Phase portraits when $r_1 = 1$ depict the worldwide sink at $s_2 = (0,1.53)$. (c) Direction field when $r_1 = 2$. (d) Phase portraits when $r_1 = 2$ depict

the bistable behavior between s_2 and s_{32}. (e) Direction field when $r_1 = 3.2$. (f) Phase portraits when $r_1 = 3.2$ depict worldwide sink at $s_3 = (12.7,1.74)$. (g) Direction field when $r_1 = 3.65$. (h) Phase portraits when $r_1 = 3.65$ depict worldwide sink at $s_1 = (20.28,0)$.

An investigation of the role of n on the dynamic of system (5) with parameters (34) was done numerically and the following results are obtained. For $n \leq 1.43$ system (5) has three boundary points $s_0, s_1 = (10.85,0)$ and $s_2 = (0,1.53)$ which are source, saddle, and worldwide sink respectively. However, for $n > 1.43$ two co-existing equilibrium points appear in addition the boundary points and the system undergoes a bistable between s_2 and s_{32}. It is observed that the first co-existing point s_{31} gradually approached to s_2 as n increases and the system eventually transfers to worldwide sink at a unique co-existing point, see Figures (2d) for $n = 2$ and Figure (3d) for $n = 10$. To explain the above-obtained results, Figure (3) is obtained using numerical solution of the system (5) for parameters (34) with the selected values of n.

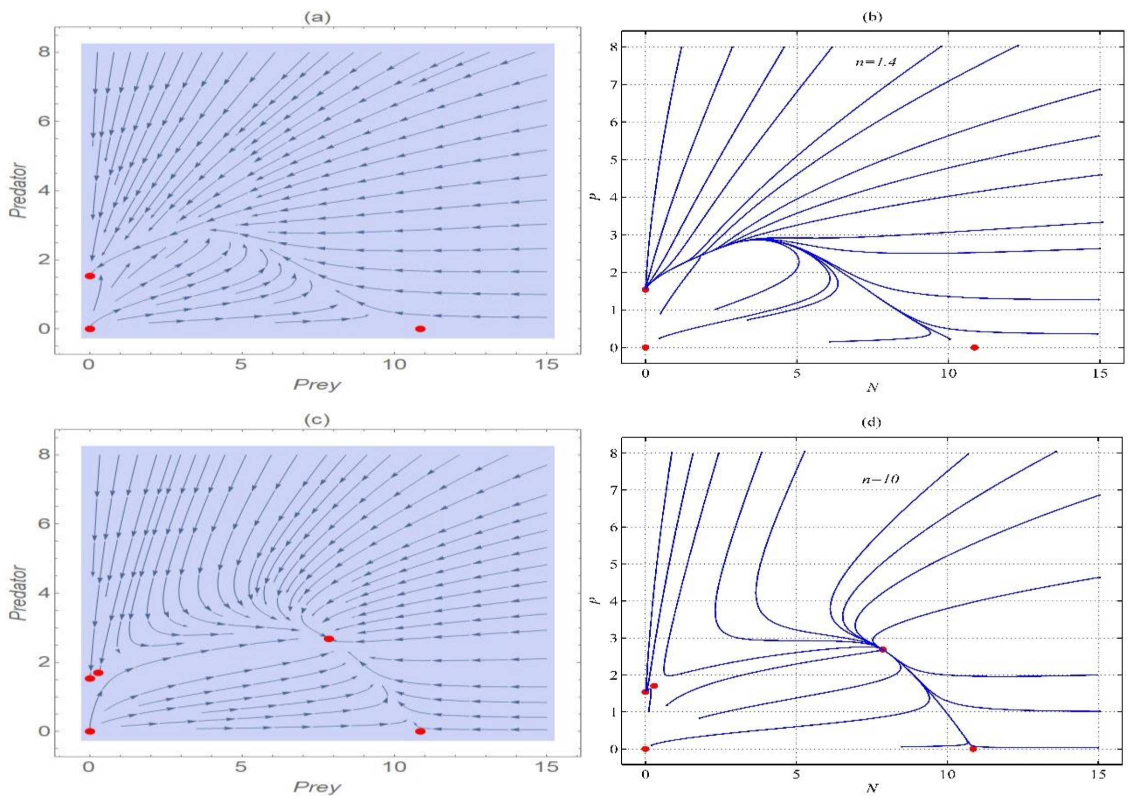

Fig. 3: (a) Direction field when $n = 1.4$. (b) Phase portraits when $n = 1.4$ depict the worldwide sink at $s_2 = (0,1.53)$. (c) Direction field when $n = 10$. (d) Phase portraits when $n = 10$ depict the bistable behavior between $s_2 = (0,1.53)$ and $s_{32} = (7.85,2.68)$ with approaching of $s_{31} = (0.28,1.7)$ to s_2 as n increases.

An investigation of the role of m on the dynamic of system (5) was done using numerical simulation. To is obtained that, for $m \leq 0.42$, system (5) has only boundary points with s_2 is a worldwide sink. However, for $0.42 < m \leq 1$, two co-existing point were born in addition to the three boundary points and the system undergoes a bistable behavior.

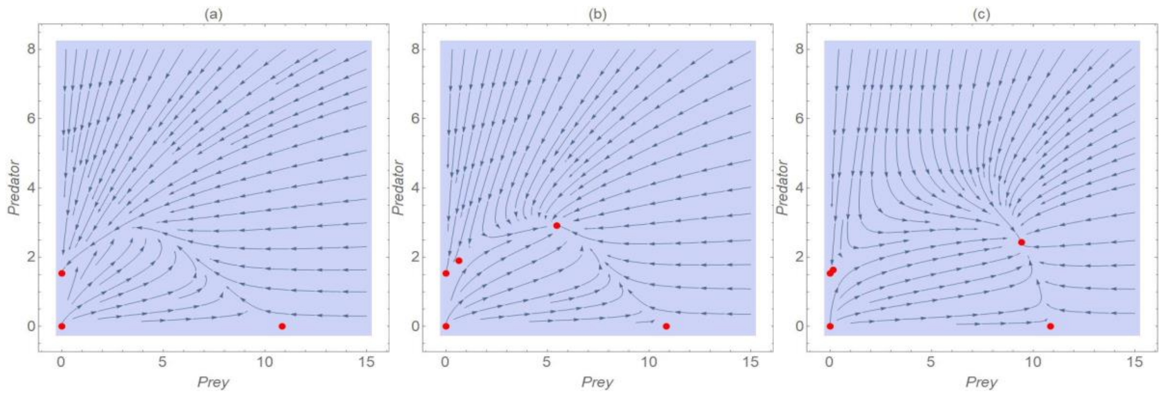

Fig. 4: Direction fields of system (5): (a) When $m = 0.4$. (b) When $m = 0.6$. (c) When $m = 0.99$.

The influence of varying b on the dynamic of system (5) is investigated numerically. The following results were obtained. For $b \leq 0.01$ the system (5) has the four equilibrium points s_0, s_1, s_2 and s_3 and it has bistable between s_1 and s_2, while s_0 is a source and s_3 saddle point. For $0.01 < b < 0.15$ two co-existing point were born in system (5) in addition to the three boundary points and the system undergoes a bistable behavior between s_2 and s_{32} as shown in Figure (2c)-(2d) when $b = 0.1$. Finally, for $b \geq 0.15$, the co-existing points disappear and the solution of system (5) approaches s_2. The above results are shown in Figure (5) using parameters (34) with selected values of b.

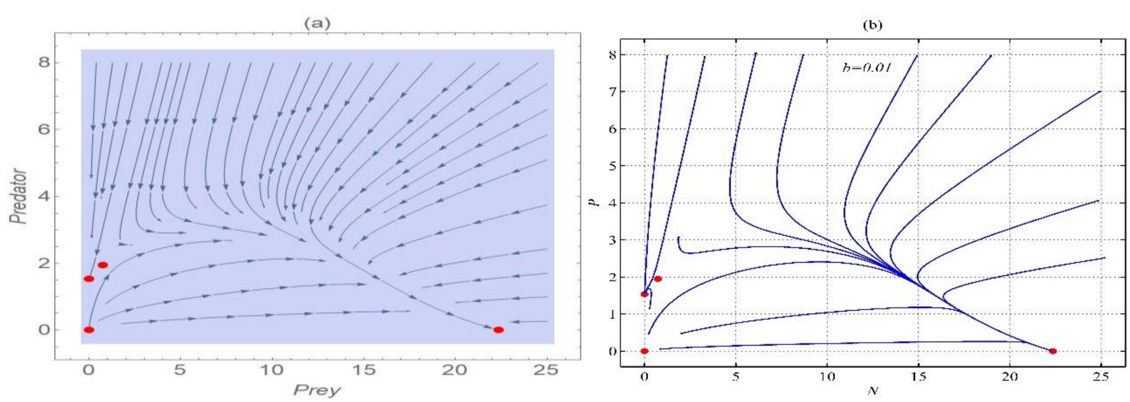

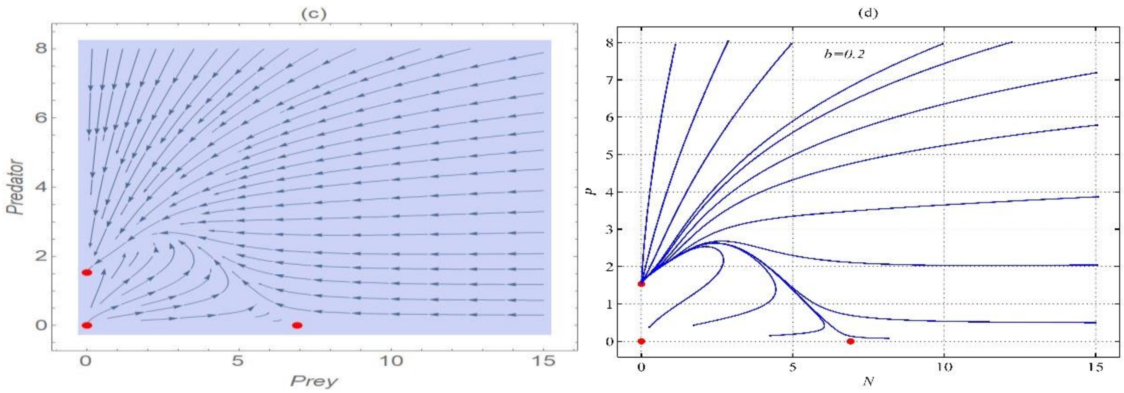

Fig. 5: (a) Direction field when $b = 0.01$. (b) Phase portraits when $b = 0.01$ depict bistable behavior between $s_1 = (22.35,0)$ and $s_2 = (0,1.53)$. (c) Direction field when $b = 0.2$. (d) Phase portraits when $b = 0.2$ depict the worldwide sink at $s_2 = (0,1.53)$.

The role of d_1 on the dynamic of system (5) in studied numerically and the obtained results give the following. For $d_1 \leq 0.18$ system (5) has two co-existing points with three boundary points and undergoes a bistable dynamic between s_2 and s_{32} while the other points are unstable, see Figure (2c)-(2(d) when $d_1 = 0.1$. However, for $0.18 < d_1 < 1$, the co-existing points disappear from the system and only three boundary points are there, where s_2 is a worldwide sink. Figure (6) shows these results at a specific value of d_1.

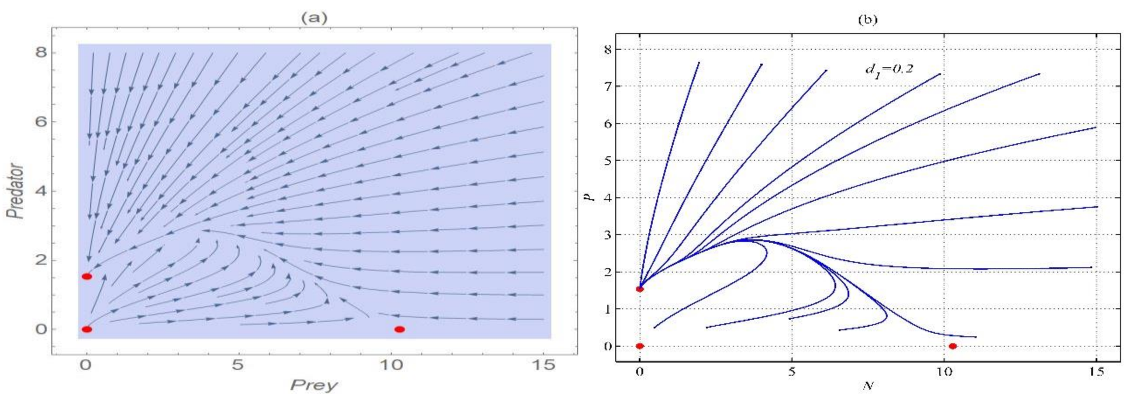

Fig. 6: (c) Direction field when $d_1 = 0.2$. (d) Phase portraits when $d_1 = 0.2$ depict the worldwide sink at $s_2 = (0,1.53)$.

It is observed that, the parameter q_1 has similar influence of the dynamic of system (5) with different bifurcation positions as that obtained with d_1, see Table (2) below.

The impact of varying the parameter a on the dynamics of the system (5) is studied numerically and the results show that, for $a \in (0,0.38]$, $a \in (0.38,0.92)$, and $a \geq 0.92$ the system (5) has a unique co-existing equilibrium point s_3, two co-existing equilibrium points s_{31} with s_{32}, and not co-existing equilibrium points, respectively. Moreover, the systems have, respectively, a worldwide sink at s_3, a bistable case between s_2 and s_{32}, and worldwide sink at s_2. Some typical results are presented in Figure (7).

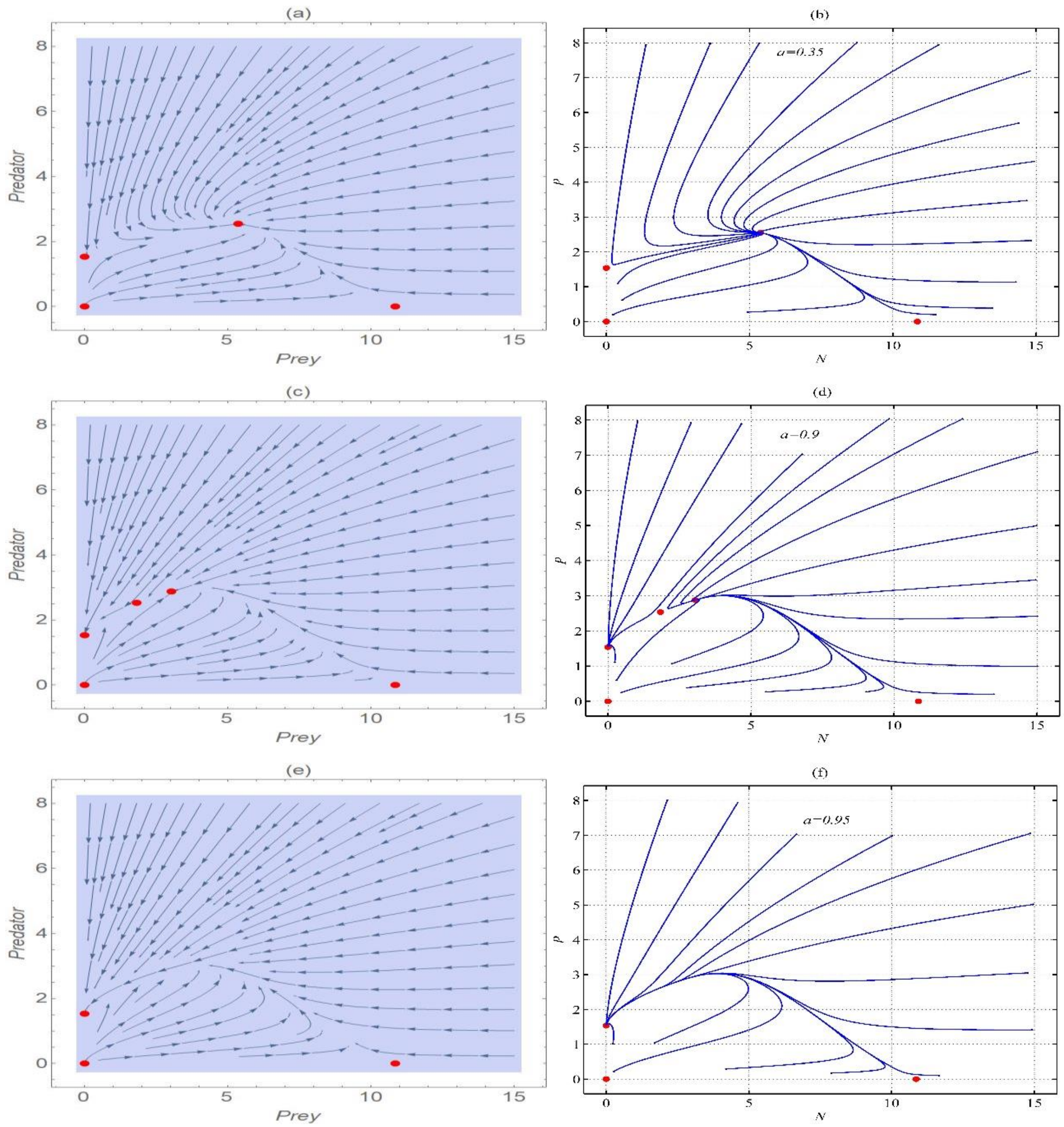

Fig. 7: (a) Direction field when $a = 0.35$. (b) Phase portraits when $a = 0.35$ depict worldwide sink at $s_3 = (5.38,2.54)$. (c) Direction field when $a = 0.9$. (d) Phase portraits when $a = 0.9$ depict the bistable behavior between $s_2 = (0,1.53)$ and $s_{32} = (3.04,2.88)$. (e) Direction field when $a = 0.95$. (f) Phase portraits when $a = 0.95$ depict worldwide sink at $s_2 = (0,1.53)$.

It is observed that, the parameter h and K have similar influence of the dynamic of system (5) with different bifurcation positions as that obtained with a, see Table (2) below.

Now, the role of c_1 on the dynamic of system (5) is investigated numerically and the following results were obtained. For the ranges $c_1 \in (0,0.1]$, $c_1 \in (0.1,0.89]$, and $c_1 > 0.89$ system (5) have three boundary equilibrium points s_0, s_1, and s_2 with s_2 is worldwide sink, two co-existing equilibrium points s_{31}, s_{32} in addition to the boundary points with bistable behavior between s_2 and s_{32} see Figures (2c)-(2d) for an explain, and a unique co-existing equilibrium point s_3 in addition to the three boundary points with worldwide sink at s_3 respectively. Figure (8) explains these results for selected values of c_1.

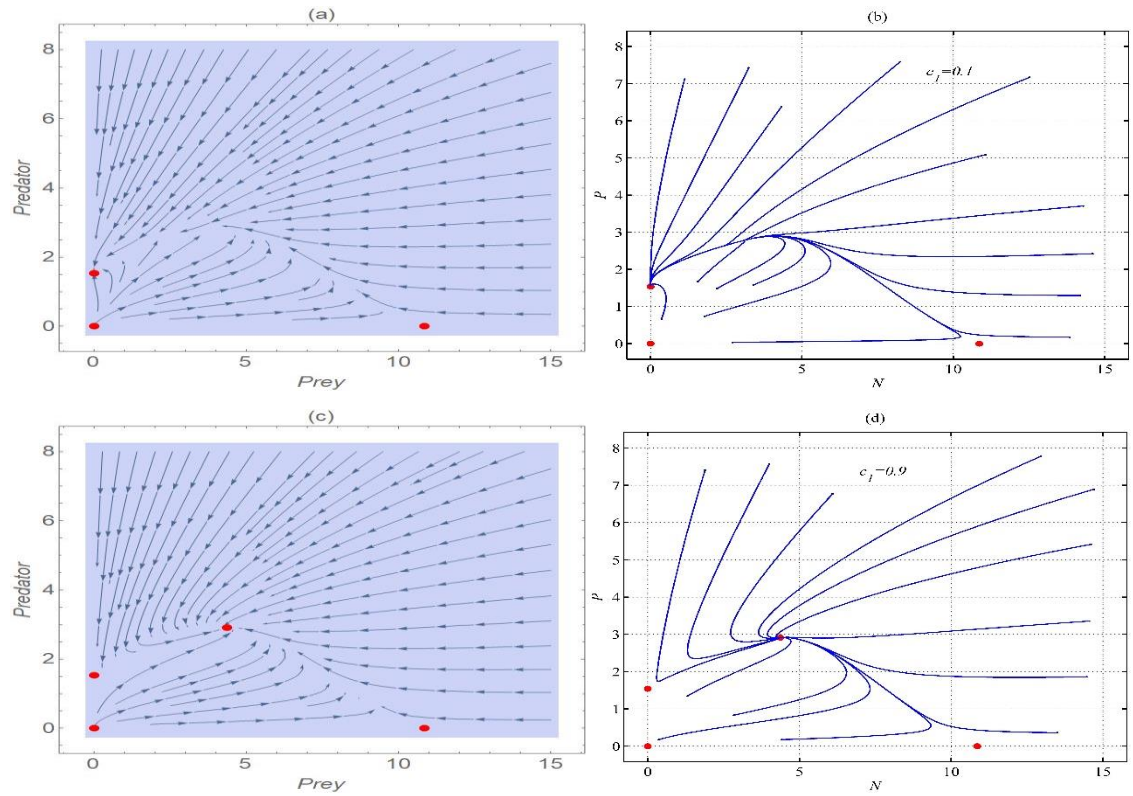

Fig. 8: (a) Direction field when $c_1 = 0.1$. (b) Phase portraits when $c_1 = 0.1$ depict worldwide sink at $s_2 = (0,1.53)$. (e) Direction field when $c_1 = 0.9$. (f) Phase portraits when $c_1 = 0.9$ depict the worldwide at $s_3 = (4.36,2.91)$.

Similar behaviors have been obtained, as those shown in the case of varying c_1 in the system (5) when the parameters c_2, q_2, and E are varying with different bifurcating positions, see Table (2).

A study using numerical simulation for the influence of the parameter r_2 on the dynamic of the system (5) has been carried out. It is obtained that, for the $r_2 \leq 0.35$ the system has only three boundary equilibrium points s_0, s_1, and s_2 with s_1 being the worldwide sink. For $0.35 < r_2 \leq$

0.54 a unique co-existing equilibrium point s_3 is born but the system (5) still has a worldwide sink at s_1. However, for the range $0.54 < r_2 \leq 1.11$ two co-existing equilibrium points s_{31}, s_{32} have appeared in addition to the three boundary points and the system (5) has a bistable case, see Figures (2c)-(2d) for explain. Finally, for $r_2 > 1.11$ the system (5) has only three boundary equilibrium points with a worldwide sink at s_2. To explain the obtained results, Figure (9) is drawn for some selected values of r_2.

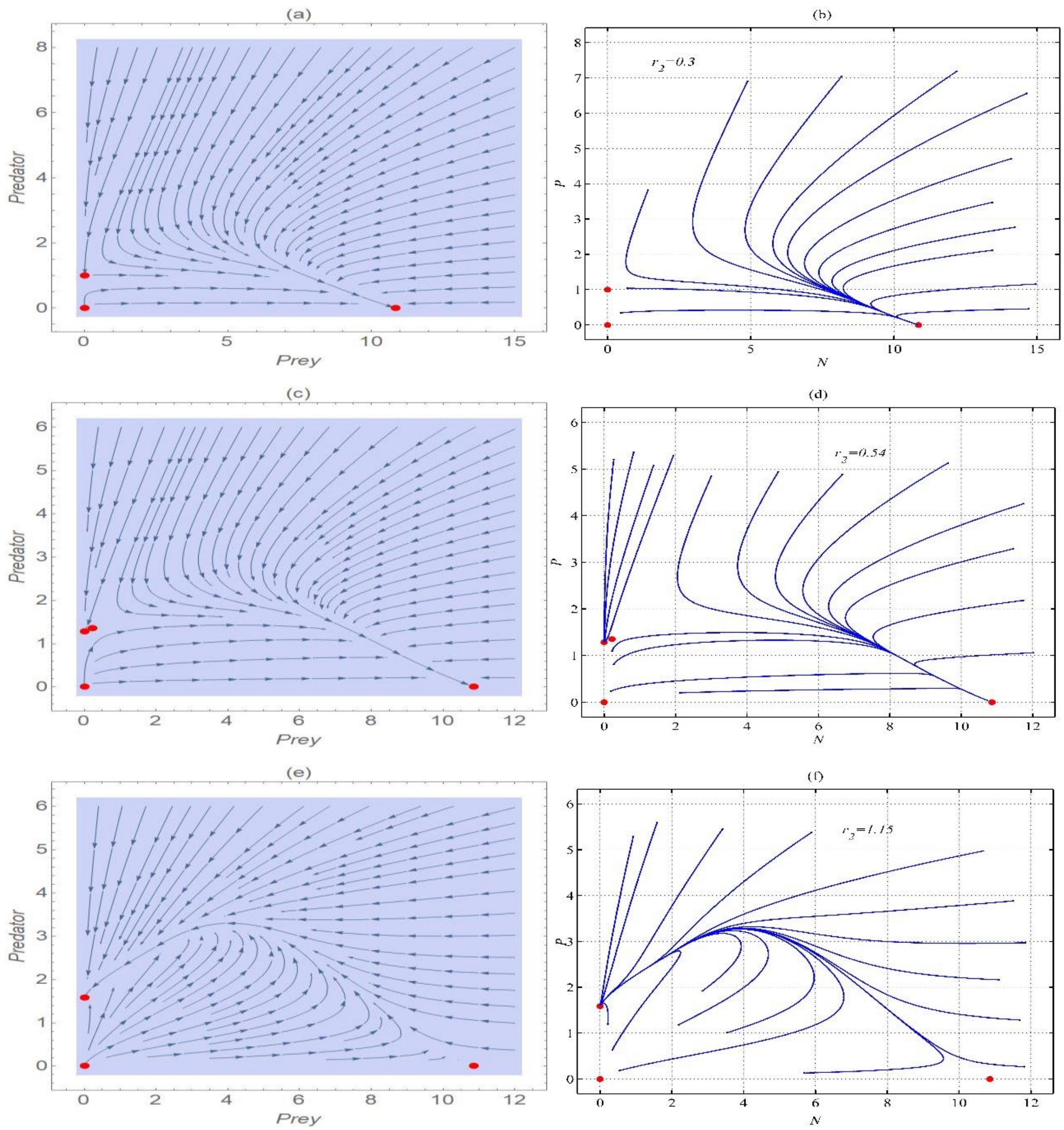

Fig. 9: (a) Direction field when $r_2 = 0.3$. (b) Phase portraits when $r_2 = 0.3$ depict worldwide sink at $s_1 = (10.85,0)$. (c) Direction field when $r_2 = 0.54$. (d) Phase portraits when $r_2 = 0.54$

depict the bistable behavior between $s_1 = (10.85,0)$ and $s_2 = (0,1.28)$. (e) Direction field when $r_2 = 1.15$. (f) Phase portraits when $r_2 = 1.15$ depict worldwide sink at $s_2 = (0,1.53)$.

Finally, the role of varying d_2 on the dynamic of system (5) is investigated numerically and the following results are obtained. For the range $d_2 \leq 0.02$ the system have three boundary equilibrium points s_0, s_1, and s_2 with s_2 being the worldwide sink. For the range $0.02 < d_2 < 0.1$ two co-existing equilibrium points s_{31}, s_{32} have appeared in addition to the three boundary points and the system (5) has a bistable case, see Figures (2c)-(2d) for explain. However, for the range $0.1 \leq d_2 < 1$ a unique co-existing equilibrium point s_3 is born and the system (5) has a bistable behavior between s_1 and s_2. To explain these obtained results Figure (10) at selected values of d_2 is given.

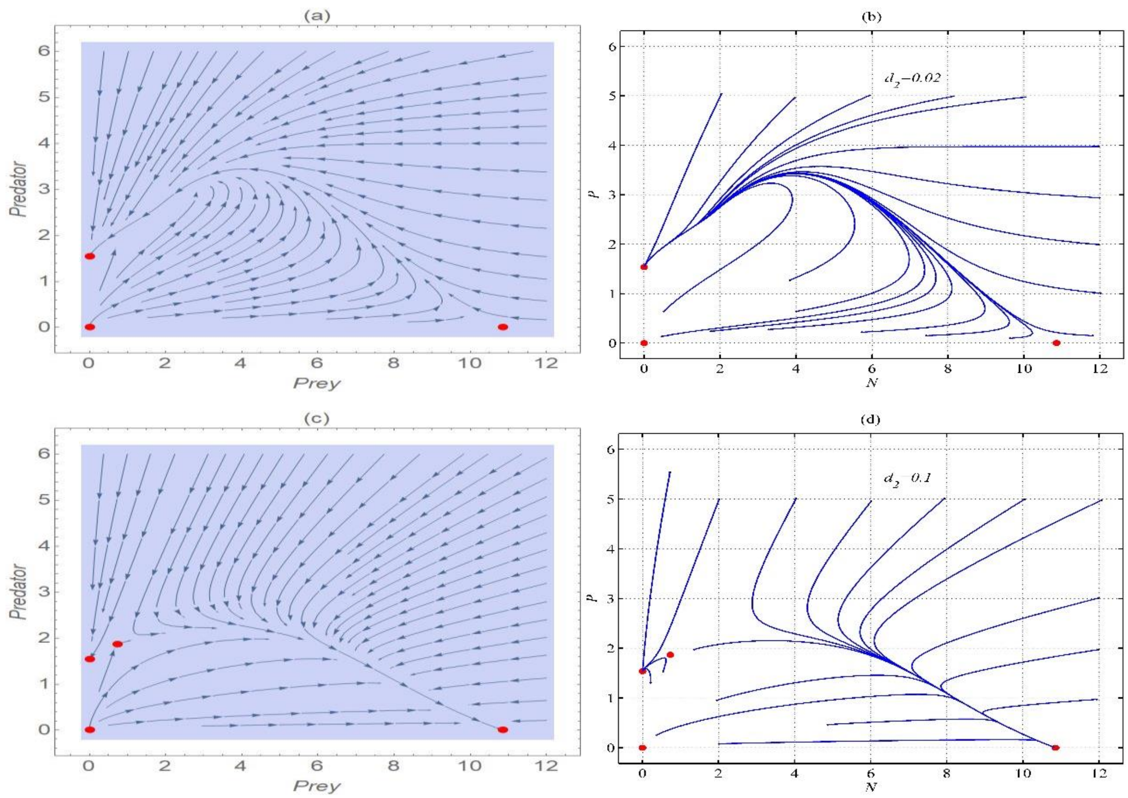

Fig. 10: (a) Direction field when $d_2 = 0.02$. (d) Phase portraits when $d_2 = 0.02$ depict the worldwide sink at $s_2 = (0,1.53)$. (c) Direction field when $d_2 = 0.1$. (d) Phase portraits when $d_2 = 0.1$ depict bistable behavior between $s_1 = (10.85,0)$ and $s_2 = (0,1.53)$.

Table 2: The dynamical behavior of system (5) as a function of parameters.

The parameter	Range	The existence equilibrium points	The system dynamical behavior
q_1	$q_1 \in (0,0.15]$	$s_0,\ s_1,\ s_2,\ s_{31},\ s_{32}$	Bistable between s_2 and s_{32}
	$q_1 > 0.15$	$s_0,\ s_1,\ s_2$	Worldwide sink at s_2
h	$h \in (0,0.01]$	$s_0,\ s_1,\ s_2,\ s_3$	Worldwide sink at s_3
	$h \in (0.01,0.31]$	$s_0,\ s_1,\ s_2,\ s_{31},\ s_{32}$	Bistable between s_2 and s_{32}
	$h > 0.31$	$s_0,\ s_1,\ s_2$	Worldwide sink at s_2
K	$K \in (0,1.29]$	$s_0,\ s_1,\ s_2,\ s_3$	Worldwide sink at s_3
	$K \in (1.29,2.67]$	$s_0,\ s_1,\ s_2,\ s_{31},\ s_{32}$	Bistable between s_2 and s_{32}
	$K > 2.67$	$s_0,\ s_1,\ s_2$	Worldwide sink at s_2
c_2	$c_2 \in (0,0.05]$	$s_0,\ s_1,\ s_2$	Worldwide sink at s_2
	$c_2 \in (0.05,0.44]$	$s_0,\ s_1,\ s_2,\ s_{31},\ s_{32}$	Bistable between s_2 and s_{32}
	$c_2 > 0.44$	$s_0,\ s_1,\ s_2,\ s_3$	Worldwide sink at s_3
q_2	$q_2 \in (0,0.17]$	$s_0,\ s_1,\ s_2$	Worldwide sink at s_2
	$q_2 \in (0.17,0.57)$	$s_0,\ s_1,\ s_2,\ s_{31},\ s_{32}$	Bistable between s_2 and s_{32}
	$q_2 \geq 0.57$	$s_0,\ s_1,\ s_2,\ s_3$	Worldwide sink at s_3
E	$E \in (0,0.62]$	$s_0,\ s_1,\ s_2$	Worldwide sink at s_2
	$E \in (0.62,2.1]$	$s_0,\ s_1,\ s_2,\ s_{31},\ s_{32}$	Bistable between s_2 and s_{32}
	$E > 2.1$	$s_0,\ s_1,\ s_2,\ s_3$	Worldwide sink at s_3

7. CONCLUSIONS

A prey-predator model involving hunting cooperation and antipredator behavior is proposed and studied in this paper. The modified Leslie–Gower type of interaction is adopted in the growth of predators, and the fear impact on the dynamic of the system is included too. It is assumed there are harvesting process is imposed on the system too. All the characteristic properties of the solution, including positivity and boundedness are discussed. The system have at most three boundary equilibrium points and co-existing equilibrium point that is whenever exist it is unique under certain conditions. The stability analysis, uniform persistence, and local bifurcation analysis are performed to understand the system dynamics.

A numerical example is given to further understand the influence of varying the parameters of the system and confirm the obtained analytical findings. It is observed through the numerical simulations the following. The system is rich in the dynamic behavior so that it includes many ranges for all parameters with bistablility case behavior in which the system approach for the same set of parameters with different initial values to two different attractors. The system does not have periodic dynamics. The fear has a stabilizing influence on the dynamic of the system. The hunting cooperation coefficients a and h have an extinction impact on the system and the solution approach to the prey-free point. The half saturation constant c_1, the catchability coefficient of the predator q_2, the harvesting effort E, and the level of interference between the individuals of a predator c_2 have stabilizing effects on the system dynamic. All other parameters have an extinction effect on the system.

CONFLICT OF INTERESTS

The author declares that there is no conflict of interests.

REFERENCES

[1] A. A. Berryman, A. P. Gutierrez and R. Arditi, Credible, Parsimonious and Useful Predator-Prey Models: A Reply to Abrams, Gleeson, and Sarnelle, Ecology, 76 (1995), 1980-1985. https://www.jstor.org/stable/1940728.

[2] R.M. May, Stability and complexity in model ecosystems, 2nd ed., Princeton University Press, Princeton, 2001.

[3] A.D. Bazykin, A.I. Khibnik, B. Krauskopf, Nonlinear dynamics of interacting populations, World Scientific, Singapore, 1998. https://doi.org/10.1142/2284.

[4] J.D. Murray, Mathematical biology, Springer, New York, 1989.

[5] P.H. Leslie, Some further notes on the use of matrices in population mathematics, Biometrika. 35 (1948), 213-245. https://doi.org/10.1093/biomet/35.3-4.213.

[6] M.A. Aziz-Alaoui, M. Daher Okiye, Boundedness and global stability for a predator-prey model with modified Leslie-Gower and Holling-type II schemes, Appl. Math. Lett. 16 (2003), 1069-1075. https://doi.org/10.1016/s0893-9659(03)90096-6.

[7] E. Gonzalez-Olivares, A. Rojas-Palma, Global stability in a modified Leslie-Gower type predation model assuming mutual interference among generalist predators, Math. Biosci. Eng. 17 (2020), 7708-7731. https://doi.org/10.3934/mbe.2020392.

[8] S.M.A. Al-Momen, R.K. Naji, The dynamics of modified Leslie-Gower predator-prey model under the influence of nonlinear harvesting and fear effect, Iraqi J. Sci. 63 (2022), 259-282. https://doi.org/10.24996/ijs.2022.63.1.27.

[9] A.R.M. Jamil, R.K. Naji, Modeling and analyzing the influence of fear on the harvested modified Leslie-Gower model, Baghdad Sci. J. (2023). https://doi.org/10.21123/bsj.2023.7432.

[10] A.R.M. Jamil, R.K. Naji, Modeling and analysis of the influence of fear on the harvested modified Leslie-Gower model involving nonlinear prey refuge, Mathematics. 10 (2022), 2857. https://doi.org/10.3390/math10162857.

[11] M.A. Elgar, Predator vigilance and group size in mammals and birds: a critical review of the empirical evidence, Biol. Rev. 64 (1989), 13-33. https://doi.org/10.1111/j.1469-185x.1989.tb00636.x.

[12] Z. Abramsky, M.L. Rosenzweig, A. Subach, The costs of apprehensive foraging, Ecology. 83 (2002), 1330-1340. https://doi.org/10.1890/0012-9658(2002)083[1330:tcoaf]2.0.co;2.

[13] E.L. Preisser, D.I. Bolnick, The many faces of fear: comparing the pathways and impacts of nonconsumptive predator effects on prey populations, PLoS ONE. 3 (2008), e2465. https://doi.org/10.1371/journal.pone.0002465.

[14] X. Wang, L. Zanette, X. Zou, Modelling the fear effect in predator-prey interactions, J. Math. Biol. 73 (2016), 1179-1204. https://doi.org/10.1007/s00285-016-0989-1.

[15] X. Wang, X. Zou, Modeling the fear effect in predator-prey interactions with adaptive avoidance of predators, Bull. Math. Biol. 79 (2017), 1325-1359. https://doi.org/10.1007/s11538-017-0287-0.

[16] S. Pal, S. Majhi, S. Mandal, et al. Role of fear in a predator-prey model with Beddington-DeAngelis functional response, Z. Naturforsch. A. 74 (2019), 581-595. https://doi.org/10.1515/zna-2018-0449.

[17] N.H. Fakhry, R.K. Naji, The dynamics of a square root prey-predator model with fear, Iraqi J. Sci. 61 (2020), 139-146. https://doi.org/10.24996/ijs.2020.61.1.15.

[18] S.K. Sasmal, Y. Takeuchi, Dynamics of a predator-prey system with fear and group defense, J. Math. Anal. Appl. 481 (2020), 123471. https://doi.org/10.1016/j.jmaa.2019.123471.

[19] F.H. Maghool, R.K. Naji, The dynamics of a tritrophic Leslie-Gower food-web system with the effect of fear, J. Appl. Math. 2021 (2021), 2112814. https://doi.org/10.1155/2021/2112814.

[20] S. Vinoth, R. Sivasamy, K. Sathiyanathan, et al. The dynamics of a Leslie type predator-prey model with fear and Allee effect, Adv. Differ. Equ. 2021 (2021), 338. https://doi.org/10.1186/s13662-021-03490-x.

[21] N. Santra, S. Mondal, G. Samanta, Complex dynamics of a predator-prey interaction with fear effect in deterministic and fluctuating environments, Mathematics. 10 (2022), 3795. https://doi.org/10.3390/math10203795.

[22] F.H. Maghool, R.K. Naji, Chaos in the three-species Sokol-Howell food chain system with fear, Commun. Math. Biol. Neurosci. 2022 (2022), 14. https://doi.org/10.28919/cmbn/7056.

[23] L. Ji, C. Wu, Qualitative analysis of a predator-prey model with constant-rate prey harvesting incorporating a constant prey refuge, Nonlinear Anal.: Real World Appl. 11 (2010), 2285-2295. https://doi.org/10.1016/j.nonrwa.2009.07.003.

[24] Md. Manarul Haque, S. Sarwardi, Dynamics of a harvested prey-predator model with prey refuge dependent on both species, Int. J. Bifurcation Chaos. 28 (2018), 1830040. https://doi.org/10.1142/s0218127418300409.

[25] H.A. Satar, R.K. Naji, Stability and bifurcation of a prey-predator-scavenger model in the existence of toxicant and harvesting, Int. J. Math. Math. Sci. 2019 (2019), 1573516. https://doi.org/10.1155/2019/1573516.

[26] A.S. Abdulghafour, R.K. Naji, A study of a diseased prey-predator model with refuge in prey and harvesting from predator, J. Appl. Math. 2018 (2018), 2952791. https://doi.org/10.1155/2018/2952791.

[27] M.T. Alves, F.M. Hilker, Hunting cooperation and Allee effects in predators, J. Theor. Biol. 419 (2017), 13-22. https://doi.org/10.1016/j.jtbi.2017.02.002.

[28] J. Zhang, W. Zhang, Dynamics of a predator-prey model with hunting cooperation and Allee effects in predators, Int. J. Bifurcation Chaos. 30 (2020), 2050199. https://doi.org/10.1142/s0218127420501990.

[29] H.A. Satar, R.K. Naji, Stability and bifurcation in a prey-predator-scavenger system with Michaelis-Menten type of harvesting function, Differ. Equ. Dyn. Syst. 30 (2019), 933-956. https://doi.org/10.1007/s12591-018-00449-5.

[30] J. Liu, B. Liu, P. Lv, et al. An eco-epidemiological model with fear effect and hunting cooperation, Chaos Solitons Fractals. 142 (2021), 110494. https://doi.org/10.1016/j.chaos.2020.110494.

[31] N.H. Fakhry, R.K. Naji, The dynamic of an eco-epidemiological model involving fear and hunting cooperation, Commun. Math. Biol. Neurosci. 2023 (2023), 63. https://doi.org/10.28919/cmbn/7998.

[32] I.M. Graham, X. Lambin, The impact of weasel predation on cyclic field-vole survival: the specialist predator hypothesis contradicted, J. Anim. Ecol. 71 (2002), 946-956. https://doi.org/10.1046/j.1365-2656.2002.00657.x.

[33] R.P. Gupta, P. Chandra, Bifurcation analysis of modified Leslie-Gower predator–prey model with Michaelis-Menten type prey harvesting, J. Math. Anal. Appl. 398 (2013), 278-295. https://doi.org/10.1016/j.jmaa.2012.08.057.

[34] S. Yu, Global stability of a modified Leslie-Gower model with Beddington-DeAngelis functional response, Adv. Differ. Equ. 2014 (2014), 84. https://doi.org/10.1186/1687-1847-2014-84.

[35] A.K. Pal, Effect of fear on a modified Lesli-Gower predator-prey eco-epidemiological model with disease in predator, J. Appl. Math. Inform. 38 (2020), 375-406. https://doi.org/10.14317/JAMI.2020.375.

[36] A. Singh, P. Malik, Bifurcations in a modified Leslie-Gower predator-prey discrete model with Michaelis-Menten prey harvesting, J. Appl. Math. Comput. 67 (2021), 143-174. https://doi.org/10.1007/s12190-020-01491-9.

[37] K. Sarkar, S. Khajanchi, Impact of fear effect on the growth of prey in a predator-prey interaction model, Ecol. Complex. 42 (2020), 100826. https://doi.org/10.1016/j.ecocom.2020.100826.

[38] E. González-Olivares, B. González-Yañez, R. Becerra-Klix, et al. Multiple stable states in a model based on predator-induced defenses, Ecol. Complex. 32 (2017), 111-120. https://doi.org/10.1016/j.ecocom.2017.10.004.

[39] L. Perko, Differential equations and dynamical systems, 3rd ed., Springer, New York, 2001.

[40] F. Chen, On a nonlinear nonautonomous predator-prey model with diffusion and distributed delay, J. Comput. Appl. Math. 180 (2005), 33-49. https://doi.org/10.1016/j.cam.2004.10.001.